ADDIS ABABA UNIVERSITY
SCHOOL OF GRADUATE STUDIES

APPLICATION OF INTEGREATED GEOPHYSICAL METHODS FOR THE EVALUATION OF THERMAL CENTERS AND THEIR STRUCTURAL CONTROLS IN BOKU,NAZARETH, MAIN ETHIOPIAN RIFT

BERHANU MENGISTU
MAY 1999

APPLICATION OF INTEGERATED GEOPHYSICAL METHODS FOR THE EVALUATION OF THERMAL CENTERS AND THEIR STRUCTURAL CONTROLS IN BOKU,NAZARETH, MAIN ETHIOPIAN RIFT

By

BERHANU MENGISTU

A Thesis submitted to the

School of Graduate Studies

Addis Ababa University

In Partial Fulfilment of

The Requirements of the Degree

Master of Science in Exploration Geophysics

May 1999

ABSTRACT

In this work combined Vertical Electrical Sounding (VES), Dipole-Dipole profiling and magnetic surveys are carried out around the Boku thermal area near Nazareth town. The analysis of the results obtained from the integrated geophysical methods has provided useful information regarding the electrical characteristics of the subsurface, which is related to the thickness and depth ranges of the different subsurface layers. The physical property distribution, which is obtained by these surveys, is analysed with particular significance for thermal water and structural controls.

Nine Vertical Electrical Sounding (VES) measurements using the Schulumberger configuration along two parallel profiles were carried out. The field apparent resistivity data is plotted against electrode separation and initial model parameters for each sounding station are obtained using two layer master curves and the auxiliary point charts. For quantitative evaluation of the resistivity soundings, the field data were fed to an iterative computer program. In this program the apparent resistivities obtained as a function of electrode spacings are converted to true resistivities as a function of depth. Using the initial model parameters obtained from curve matching, the computer program iteratively modifies the resistivities to obtain the best fit with the field data for the layer thickness chosen for the model.

Based on the inversion, a five-layered geoelectric section is obtained along the first profile except at VES 2, which has got a three-layer earth structure. A unique distribution of subsurface resistivity has been observed at VES 4 and on the second profile. This unique subsurface resistivity is characterised by a very low resistivity value for the large electrode separation. This behaviour may actually be associated with the high conductance of the deep layers. The location of the Boku thermal centre, which is between the position of VES 5 and 6, has a four and five layered earth structure. From the geoelectric section it is expected that a fault zone may be the

structural contact zone. A pattern of very low resistivity value is observed at the position of VES2, which is bounded by a very high resistivity value at the position of VES 1 and VES 3. A lithological contact zone may be expected around the location of VES 1 and VES 2. The same resistivity difference is observed between VES 5 and VES 6. VES 4 has shown a typical nature, which is characterised, by a very low resistive zone. To ensure the real electrical behaviour of the area an additional geophysical method such as gravity methods may be more valuable.

The second profile consists of VES 7,8 and 9 and VES 7 has a seven layered earth structure, VES 8 has a three layered earth structure and VES 9 had a four layered earth structure. Along profile 2 the interesting behaviour is the very low resistive zones for the large electrode separation which indicates the deep structural and geological features of the study area.

The dipole- dipole profiling psedosection section has been carried out only along the first profile. Here also, very low resistive zone is investigated around the location of the first segment, which is the position of VES1, 2 and 3. Also very low resistive zone is investigated around VES 5 and 6 that is the Boku thermal centre. Segment two of the profiling pseudosection generally indicates a high resistive zone.

The magnetics survey shows generally qualitative information. Avery low magnetic response is observed around the location of VES 1 for the first profile. Along the second profile a very low magnetic response is observed around the location of VES 2 and VES 5, which might be associated with the fault or fracture in the area. Again profile 3 has shown a very low magnetic response around the position of VES.

ACKNOWLEDGEMENTS

My acknowledgements goes first and for most to my advisors, **Dr Tigistu Haile and Ato Shemelis Fisseha,** whose proper guidance throughout the study and preparing all the necessary financial resource has been of paramount importance.

I am indebted to **Dr Solomon Tadesse** who arranged all the necessary field expenses of the first field trip. I would like also to express my heartfelt appreciation to my real brothers: **Ato Getu Mengistu, Ato Tesfaye Mengistu and Ato Tadesse Mengistu** who contributed a lot regarding the financial support to bring this work to an end.

My thanks also go to Ato **Biniam** and all the members of the geophysics department of the EIGS for their co-operation of the computer software facilities. The generosity of colleagues and friends has been invaluable. Especially great thanks go to my friends **Ato Sharew Gultu, Ato Berhanu Tesfaye, Ato Awoel Sherif and Ato Eyob Amide for** their advice and support to bring this work to an end.

Last but not least I would like to express my thanks to **Roza Demissie** for her continuos follow up of my personal situation to finish this work.

TABLE OF CONTENTS **PAGES**

LIST OF FIGURES

TITLE

LIST OF TABLES

1. INTRODUCTION

Geophysical methods are applied to obtain information about the subsurface of the earth that is not available from surface geological observations. A variety of natural resources, engineering and scientific applications can benefit from geophysical field surveys capable of detecting and mapping underground inhomogeneities and structures and to solve various problems in the field of applied geology and engineering. In particular the contribution of the geophysical methods in the evaluation of hydrogeological systems has been acknowledged in many parts of the world.

Geophysical exploration examines the physical phenomena of the earth, measures their associated parameters and is applied to the solution of geological problems. In the case of geothermal fields it is applied to distinguish suitable location of bore- holes through which hot fluids at depth can be tapped.

Geothermal energy is an important and promising alternative energy resource that has seen a continual growth throughout this century; regrettably, its fortunes have reflected the variable success experienced when traditional petroleum exploration techniques are used.

There is abundant geothermal energy in the earth's crust and it has the potential to make the energy economies of many countries throughout the world particularly as fossil fuels grow more expensive and scarce. Of course the use of geothermal energy already has been demonstrated in many different settings throughout the world.

There is no argument that the geothermal energy in the earth is immense and there is likewise little argument that most of this energy is far too deeply buried ever to be of practical concern in terms of extinction and use by man. But even restricting ones attention to the

geothermal energy in only the earth's crust (approximately the outer 10 - 15km) the amount of usable energy is still huge. The growth of geothermal energy use is varied in the technological and scientific areas such as electrical power generation, for space heating, process heating, agricultural use, etc. Non-electrical applications of geothermal energy are such as animal husbandry, plastic explosive manufacturing, water desalination, and snow melting milk pasteurisation and air conditioning.

Geothermal energy is also used for hydrotherapy, extraction of chemicals (both associated or not with the geothermal fluids) and for fresh water supply.

It is a common experience that areas with high anomalous thermal gradient and various forms of hydrothermal activities are expected to show anomalously high temperature at depth. These might represent exploitable and economically important concentrations if found at depths between 1/2km and 3km. Deeper sources would be costly to exploit and shallower ones have insufficient pressure to permit the high enthalpy desired (Gezahegn 1980).

In Ethiopia various areas within the rift valley have been identified to possess great potential for geothermal energy. One of these areas is the Boku fumaroles, which are located in the tectonically active central part of the Main Ethiopian Rift and are associated with the acidic central volcano which has been erupted in the late Quaternary. Since the hydrothermal activities are localised on the western shoulder of this volcano, and more specifically outside the Calder, an appropriate conceptual model is prepared to show the major hydrothermal fluid carrying structures and the associated rhyolitic structures (foliation features) which diffuse the steam at the surface. (Tamiru and Vernier, 1997). The aim of the present study is to define the major structural controls of the Boku thermal centres and test the effectiveness of the proposed model in the area where there are numerous thermal manifestations like thermal springs, fumaroles, hotgrounds, etc., using geophysical methods.

1.1 The Study Area

The study area is located in the tectonically active axial part of the East African Rift system between 8^0 23'- 8^0 32' latitude & 39^0 14'- 39^0 24' longitude where the topography is dominated by sunken strips of land between a series of normal faults. More specifically, the area is located in the part of the rift system called the Main Ethiopian Rift (MER) that occupies the central part of the country where acidic and central volcanoes are mainly erupted along NE - SW tectonic lines, Fig (1).

The area is characterised by high geothermal gradient associated with acidic volcanic centres. The main geological feature in the study area, the Boku caldera, located near Nazareth town about 100km SE of Addis Ababa, represent typical example of central eruption from where peralkaline acidic lavas and pyroclastic deposits have been erupted. This area is also characterised by high geothermal gradient and high thermal anomaly Tamiru. and Vernier, (1997). Past studies show that pyroclastic deposits are the major thermal aquifers in the lakes region, especially in the Aluto volcanic centres Berhanu (1993). On the basis of the general hydrogeological model represented in Tamiru A. and Vernier (1997), the present study will try to disclose the complex structural features of the Nazareth deep aquifer. The inclination of deep running tectonic lineaments that transport thermal waters and steam is not yet determined, which is quite important to locate precisely the source area.

The area is characterised by a repeated step faulting which makes it clear that the Boku area is still located on active deep tectonic zone. The major river flowing in the area is the Wonji Shoa River, which is located south of the Boku thermal centres.

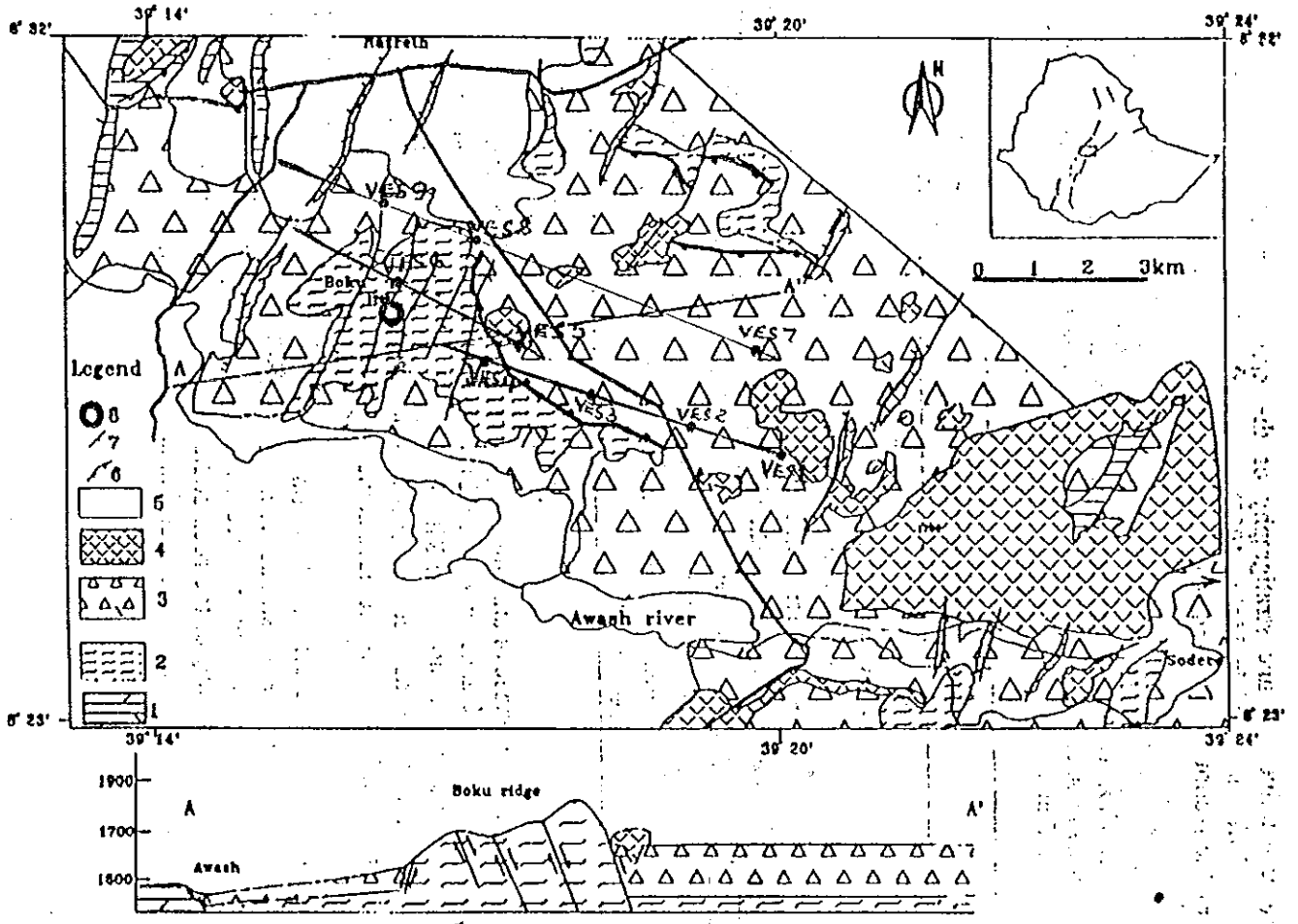

Fig. 1. Geological map of Boku area. (Modified from Alula Damte *et al.*, 1992). 1, Floor complex ignimbrites; 2, Rhyolite lava domes; 3, Unwelded ignimbrites; 4, Olivine basaltic lava flows and related spatter cones; 5, Alluvials; 6, Caldera collapse; 7, Faults; 8, Fumarole site.

1.2 Previous Work over the Area

Since the early 1970s reliable geophysical data pertaining to geothermal exploration have been obtained in the Main Ethiopian Rift. The Ethiopian institute of Geological Survey (EIGS) of the Ministry of Mines, in Cupertino with the UNDP has carried out a study of the hydrothermal activity of the area Geophysical report of the MER by UNDP (1973).

Also a report submitted by Habteab Z. and Melese B. (1987) from the EIGS of the Ministry of Mines has shown the hydrogeology and hydrochemistry of the Boku area. At the same time the same workers in the area have carried out a semi-detailed geological investigation.

The neotectonics of the Boku area has been studied by the work of Alula (1990).

Tamiru and Vernier (1997) that initiated the objective of the present study around the area have carried out a detailed hydrogeological and geochemical investigation.

All the above aspects of study collectively are interesting and they are good indication for the area to be a potential geothermal reservoir. The geophysical surveys, which form the major objective of this work, are to be presented in this paper.

1.3 Objectives of the Present Study

The aim of a geothermal exploration programme, in general, is to investigate, delineate and exploit economically attractive geothermal reservoirs characterised by high temperature (> 180°c), relatively shallow depth (< 3km), high permeability and high recharge for long term electrical and /or thermal energy production Befekadu (1989).

The objective of the present study is, based on all the geological and hydrogeological data collected so far and various geophysical methods will be carried out in the thesis work to define

the underground major structures, to locate the hot water centres and define the main circulation medium and to check the effectiveness of the proposed conceptual model for the area.

1.4 Methods of Investigation

To achieve the objective of the proposed study the following procedure has been utilised: -

First, data regarding geological and volcanological aspect of the area will be collected. These include study of the stratigraphy of the area, the relation between the hydrothermal manifestations and the structural lineaments of the area that is explained in chapter two.

Next, all the information regarding the hydrogeology and the geochemistry of the area will be gathered from published papers and interpreted to get a better future picture of the area which is discussed in chapter three.

On the third step a geophysical surveys using vertical electrical sounding, electrical profiling and magnetics method has been carried out as discussed in chapter four & five.

Finally correlation of the present study with specific literature dealing with theoretical works related with geothermal problems carried out on different places in and outside the country has been carried out in the study of the present work.

2. GEOLOGY OF THE BOKU AREA

2.1 Regional Geology of the Nazareth Area

The Ethiopian rift system which is part of the East African Rift System may be sub - divided into three main sectors. These are the South-Western Rift zone, the Main Ethiopian Rift and Afar depression.

The Main Ethiopian Rift (MER) is a symmetrical graben with uplifted flanks and steep border faults Gidey et al. (1990). This structural depression serves as a divide between the north-western or Ethiopian Plateau and the south-eastern or Somalian Plateau. According to many authors (Di Paola, 1972; Mohr, 1986;and others) this rift is the result of tensional movements which affected the uplifted Ethio-Somalia plateau. A large number of step faults have produced a total difference in altitude of more than 1000 m between the top of the plateau and the floor the rift. Almost all of these faults are normal faults (Di Paola, 1972).

The floor of the MER is marked by a persistent belt of intense, fresh, faulting which has been termed the Wonji Fault Belt (WFB) (Mohr, 1960). The WFB extends from south of Lake Chamo in southern Ethiopia to the Lake Abhe area in central Afar.

Two main tectonic events have been recognised concerning the tectonic evolution of the Ethiopian Rift System. The first event which started since Eocene (Mohr, 1976a) involved the uplift of the Ethiopian swell. Large scale faulting later took place across the swell to form the Afar and the Ethiopian Rift and this represents the second major tectonic event. The initiation of the Ethiopian Rift and the Afar can be traced to 14My ago (Kazmin and Seifemichael, 1978). (Barberi et al., 1975, and others suggest an early Miocene age for the rifts. The last major episode

of rift faulting resulted in the formation of the Wonji Fault Belt which is constituted by a number of faults which shattered the rift floor in to several relatively small horst and graben structures. According to Gidey et al. (1990) the MER may be geographically subdivided into three sectors northern, central and southern. Based on this sub- division the study area is located in the tectonically active central part of the Main Ethiopian Rift.

Di Paola (1972) identified four main successive periods of volcanic activity in the part of the MER found between 7°00'and 8°40' latitude north. Accordingly, the main events are:

1) Basaltic eruptions with emplacement of explosive dominantly ignimbritic products and associated volcano-tectonic collapses
2) Building of silicic central volcanoes on the ignimbrites
3) basaltic fissural eruptions and
4) edification of recent silicic, mostly pantelleritic, centres and associated "subhistorical" basaltic fissure eruptions.

Meyer et al., (1975) distinguished two main volcanic units in the northern part of the rift system. The first of these units is identified as the "Nazareth Series+" with an age range of 5-2 my. According to Kazmin and Seifemichael (1978), this series includes a thick succession of ignimbrites, unwelded tuffs, ash flows and rhyolitic and trachyte flows. They form the large part of the rift floor and also outcrop in the rift escarpments and on the adjacent plateau margins. In Nazareth area, according to Meyer et al .(1975), this series is represented by rhyolites and ignimbrites .Eruptions of these units is considered to be mainly through fissures and vents, but local centres also occur (Alula,1990) .

The second volcanic unit of Meyer et al.(1975), is the young "Wonji series++" built up mainly from extensive basaltic flows. Ignimbrites, rhyolite and trachyte flows, and pumice

deposits are also found in this series. his volcanisim is spatially restricted to the axial extension zone of the rift system which is the WFB. The volcanic products of this series are observed to be associated to NNE- SSE running faults or are erupted from fissures and vents in this direction (Alula,1990). The Wonji volcanism spanned from Pleistocene up to recent, according to several authors. In the Nazareth area, this series is mainly represented by basaltic and rhyolitic lava flows. The Nazareth and Wonji volcanic units are separated by a major episode of rift faulting. This faulting phase came into activity 1.6 - 1.8 my ago Kazmin and Seifemichael (1978) Mohr (1986).

The representative volcanic stratigraphy of the central part of the Main Ethiopian Rift as stated in Mohr (1983) is given in table (1), where the local stratigraphic section is also represented .

Table (1). The Nazareth area volcanic stratigaphy (Mohr, 1983 and the references therein; Alula et al., 1992). Quaternary = 0 -1.7my; Pliocene = 1.7 -5my.

Age (In millions of years)	Main Lithology	Thickness in metres
0.25	Boseti and Gadamsa Basalts Unwelded ignimbrites	≅ 3 -4 ≅ 5
0.45 -0.4	Bofa Basalts (Olivine basalts)	-
0.5	Gadamsa ignimbrites	≅ 20 - 50
0.6	Adama Boku Basalts	≅ 5
0.8	Boku Rhyolites	≅ 200
1.6	Wonji Basalts	-

1.7 -1.6	Boseti ignimbrites; floor complex ignimbrites	> 100
3.3 -3.1	Tede Rhyolites	

From stratigraphic point of view, the Boku rhyolites fall between Adama Boku basalts and Wonji basalts. The acidic rocks consist of rhyolite lava domes, obsidian flows, tuffs and ashes.

2.1.1 Stratigraphy of Nazareth area

As the work of Woldu (1994) explains the oldest volcanic rocks present in the area are represented by compact fiamme ignimbrites (I1)which show a contemporaneous emplacement with alternating flows of aphanitic dark basalt(B1). Also from places around the Nazareth area and from previous works, the I1unit is believed to be relatively older than the B1. These rocks are prominently exposed along north-Northeast oriented faults in the area west and Southwest of Nazareth town. An absolute age of 1.7my was given to the ignimbrite unit (Mohr, 1987).

Thin and subordinate layers of pyroclastic pumice fall and ash flow deposits have often been observed in sections occurring as interlayer between main flows in the above units. These pumice fall and ash flow deposits do also outcrop in few places(Woldu Ameneshoa, et al.,1994).

The above sequence is followed by rhyolitic lava flows (R1) which mainly formed the Boku Ridge and are often associated with thin obsidian interlayerings. They have also been observed to contain thin ash flow and pumice layers in some places. From absolute age data and from previous works it is believed that they are younger than the above units. An absolute age as old as 0.8 my and younger has been assigned to these rocks (Bigazzi, et al., 1981).

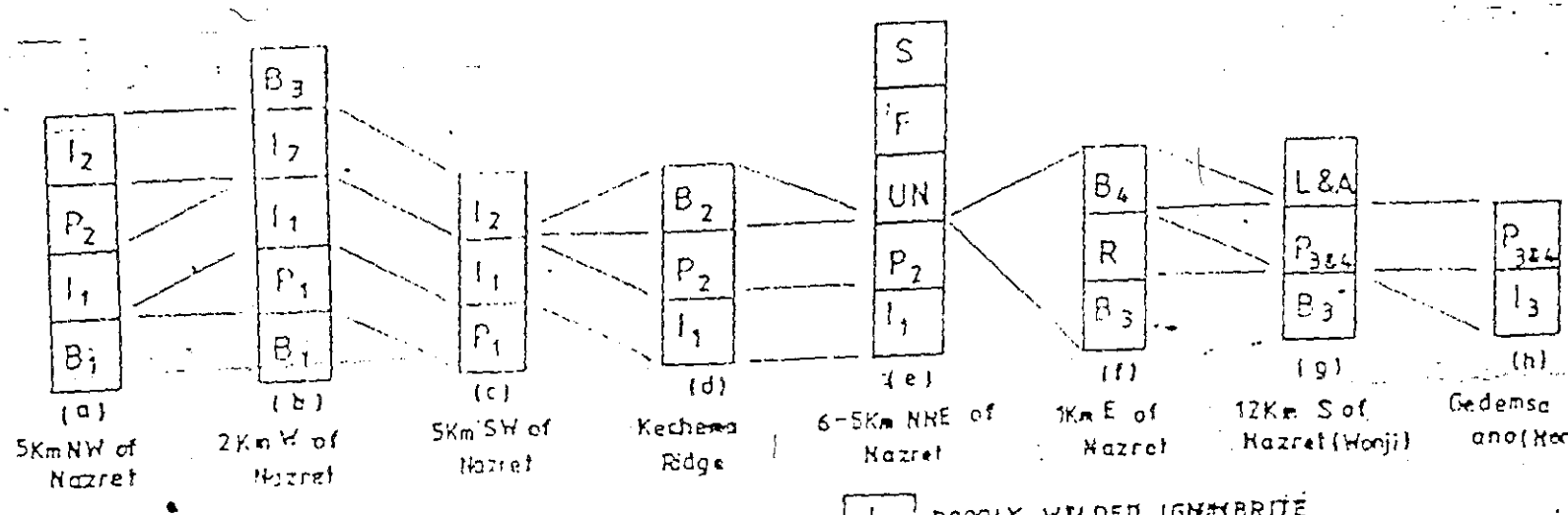

S TOP SOIL

F FLUVAL SEDIMENTS (WITH GASTROPODS & PELLETS)

UN UNWELDED TUFF (UNDERLAIN BY LEACHED SOIL)

L&A LACUSTRINE & ALLUVIAL SEDIMENTS, SOIL

B_4 BASALTIC CINDERS & SPATTERS, SCORIAS & SCORIACEOUS BASALTS

$P_{3\&4}$ UPPER PUMICE & ASH DEPOSITS (WITH SURGES)

I_3 UPPER INTENSELY WELDED IGNIMBRITE (GREEN)

R YOUNGER RHYOLITIC FLOW

B_3 PLAGIOCLASE PORPHYRY OLIVINE BASALTS

I_2 POORLY WELDED IGNIMBRITE

B_2 UPPER APHANITIC BASALT

P_2 MIDDLE PUMICE & ASH DEPOSITS

I_1 LOWER INTENSELY WELDED IGNIMBRITE (LIGHT GREEN)

P_1 LOWER PUMICE & ASH DEPOSITS

B_1 LOWER APHANITIC BASALT

FIG. • Locally Exposed Lithologic Units and Possible Stratigraphic Correlations (not to scale)

Then come the poorly welded ignimbrites (I2) with absolute age of 0.51my (Mohr,1987). The coarsely porphyritic vesicular basalt unit(B2) which is characterised by abundant feldspar and olivine phenocrysts take a stratigraphic position above the poorly welded lithic rich ignimbrites (I2) unit. An absolute age of 0.4my was assigned to this unit(Alula et al., 1992).This vesicular porphyritic basalt unit, in turn, takes a stratigraphic position below the acidic volcanics (R2)that formed the rhyolitic domes Northeast and Southwest of Nazareth, and flows east of it. Then come units that are products related to the Gadamsa caldera . They are formed by ignimbrites, ash falls and flows, pumice falls, and surges listed in a stratigraphic sequence from bottom to top as is displaced by sections in the northern part of the caldera . An absolute age range from 0.8 my to 0.2 my has been assigned to the products related to Gadamsa(Bigazzi et al., 1981).

The last phase of volcanic activity in the study area is represented by unwelded tuffs and basaltic cinder (and spatter) cones. The latter are associated with basaltic lava flows and an age younger than o.06my was given to them (Bigazzi et al.,1981).

Finally the lacustrine and fluvial sediments represent the youngest deposits in the stratigraphic sequence .Their age spanned from Pleistocene up to the present (Di Paola,1972; Kazmin and Seifemichael,1978). Table(2) shows the general stratigraphic sequence of the Nazareth area on the basis of lithologic correlation. Figure (2) shows locally exposed rock sections observed in different parts of the Nazareth area.

2.1.2 Description of Major Rock Units

In the Nazareth area reasonably good outcrops are found along ridges escarpments (in many cases bound by faults), across road cuts, river cuts and in quarries.

Table 2.1. Stratigraphic sequence of the study area.

Rock Unit	Symbol used in stra. sections	Age	Correlative unit
Lacustrine, alluvial and colluvial sediments.	L and A		
Unwelded Tuffs (with a dominant ash component)	UT		
Scoria and spatter products with associated basaltic lava flows	B_4	0.06 My (Bigazzi et al. ,1981)	Recent basalt of Kazmin et al. (1978)
Younger pyroclastic deposits (ignimbrite, pumice, ash, surge)	I_3, P_3, P_4	0.2 My and older (Bigazzi et al., 1981)	Gedemsa unit of Alula et al. (1992)
Younger rhyolitic lava flows and associated obsidian layers	R_2		Pantelleritic volcanics of Kazmin et al. (1978)
Plagioclase porphyritic olivine basalt	B_3	0.4 My (Alula et al., 1992)	Wolenchiti basalts of Meyer et al. (1975), Bofa basalts of Kazmin et al. (1978)
Poorly welded lithic rich ignimbrite	I_2	0.51 My (Mohr, 1987)	
Older rhyolitic flows & ass. obsidian layers (with pumice & ash horizons)	R_1		Older alkaline & peralkaline rhyolitic lava flows of Di Paola (1972) and others
Older pumice & ash deposits (with paleosoil horizons)	P_1 and P_2		Nazret group of Meyer (1975), Kazmin et al. (1978)
Aphanitic basalt	B_1 and B_2		Nazret group of Meyer (1975), Kazmin et al. (1978)
Intensely welded ignimbrite	I_1	1.7 My (Mohr, 1987)	Nazret group of Meyer (1975) Kazmin et al. (1978)

The rocks exposed in the area consist of various volcanics and younger sediments. The volcanics vary from basalt to rhyolite in lithology and include basaltic flows, basaltic cinder and spatter products (forming cones) acidic lava flows and ignimbrites as well as pyroclastic flows and falls (mainly pumice and ash deposits). These rocks are products of rift volcanism that spanned from Pliocene to recent (Mohr,1987 and others). While the sediments (which are lacustrine and fluvial) are of Quaternary age (Kazmin and Seifemichael, 1978; Di Paola , 1972); the fluvial sediments are present day deposits.

The rocks outcropping in the Nazareth area have been put into six units mainly based on lithologic variations, though in some cases (pyroclastic deposits) relative age relation was also considered. These lithologic units are:

a) Older pyroclastic deposits: which include poorly to intensely welded ignimbrites, ash flows and pumice fall deposits;

b) Basic lava flows (basalts): consisting of an older aphanitic basalt flow and younger porphyritic vesicular basalts;

c) Acidic lava flows: consisting of an older acidic lava flows which form the Boku Ridge (south of Nazareth) and other younger acidic products which mainly form elongated domes Northeast and Southeast of Nazareth;

d) Younger pyroclastic deposits: which include ash flows and falls, pumice falls, ignimbrites and surge deposits which are products of the Gadamsa central volcano together with much younger unwelded tuff which usually occur in many topographically low lying places;

e) Basaltic cinder and spatter products which form volcanic cones and associated basaltic lava flows; and finally

f) Reworked volcanics, lacustrine sediments, and colluvium and alluvium sediments.

2.1.3 Tectonic Features

The main geological features that have been observed in the study area include: faults, joints, and fractures (and other mesostructures like flow layering and folding associated with silicic lavas) Woldu et al (1994).

The area is intensively dissected by a number of minor and major normal faults running almost parallel to each other in a NNE-SSW direction and are usually arranged in "en echelon" fashion. These faults belong to the Wonji Fault Belt. They form steps and local graben-horst structures.

Observed downthrows estimated from the heights of the fault scarps range from few meters in the minor faults to more than 100m (mainly west of Nazareth).The faults dissect almost all units outcropping in the area and volcanism has been observed to be associated with these faults and reported to be presently buried under the lacustrine sediments (Skutan et al., 1982).

Indirect evidences of recent active faulting like very fresh fault scarps and traces of fault movement have also been observed in few places.

Joints are abundant in the intensely welded ignimbrite unit (mainly its middle portion) in the area .The unit shows fracturing and network columnar joints in the outcrops west of Nazareth. Joints and fractures (mainly concoidal) have also been observed in the other flows. Flow layering and folding have mainly been observed in the basaltic and acidic lava flow units.

2.1.4 General Geological Evolution

The eruption of the fiamme ignimbrite and the aphanitic basalt units almost contemporaneously (the latter being most probably emplaced first) occurred in the beginning.

This event is believed to be followed by a major faulting event which mainly affected the western and the southwestern parts of the area. The faulting resulted in the formation of structures like Cehema ridge. Following or together with the above faulting event occurred older acidic volcanism which gave rise to the flows that formed the Boku ridge . These volcanics were also highly affected by major faulting. Then comes the emplacement of the poorly welded lithic rich ignimbrites unit in the previously formed troughs and hence it presently occupies relatively lower topographic areas. Next occurred minor faulting events which formed small cliffs and step faults in the area. The fissure basalt eruptions which gave rise to the porphyritic vesicular basalts were related to these faulting .This was likely followed by the eruption of younger acidic volcanics which most probably occurred along previously formed faults. These acidic volcanics formed flow units and domes (the Debits and Magyar domes). The formation of the precalderal volcanics, the formation of the caldera itself and the deposition of the post calderal volcanics at Gadamsa took place at this stage . The eruption of younger scoraceous basalts and scoria (and associated flows) forming spatter and cinder cones occurred earlier and contemporaneously with the deposition of lacustrine, alluvial and colluvial sediments in the study area .The alluvial sediments represent the youngest deposition unit in the area; being present day deposit.

2.2 Detail Geology of the Boku area

Boku is between Nazareth and Wonji, about 5km south of Nazareth. Here rhyolite domes have been extruded from north-north east trending faults and subsequently displaced by faults of north-Northwest trend two areas of warm ground, both associated with the north - west faults are known. At Boku, hydrothermally altered ground extends from 200meters along the fault downthrown northeast.

East from Boku about 1km, another zone of hydrothermal alteration up to 100 metres wide extends for 300 metres along a southwest downthrown fault. At both localities chalcedony and agate are common. Calcite ,gypsum and oolitic silica are also reported.

The general geology of the area comprises of alluvium and lacustrine sediments, older alkaline and peralkaline rhyolite domes or flows of Nazareth group volcanics, and Pleistocene - subrecent basalts of the Wonji group. Locally ash and tuffs are common .The older alkaline and peralkaline rhyolite domes and flows occupying the largest area of the volcanics are composed of rhyolite and minor obisidian . The Pleistocene subrecent basalts are exposed north and east of Boku ridge on both sides of Nazareth - Asela road. The alluvium and lacustrine sediments mainly occupy lower topography areas in the surrounding of Nazareth and Wonji sugar -estate .

Boku volcanic ridge is made of alkaline and peralkaline rhyolite lava domes and flow (0.8my, Alula D. et al., 1992) which cover the floor complex ignimbrites in the central part of the rift (Fig 2). From stratigraphic point of view, the Boku rhyolites fall between Adama-Boku basalts and Wonji basalts. The acidic rocks consist of rhyolite lava domes, obsidian flows, tuffs and ashes.

The occurrence of repeated step faulting makes it clear that the Boku hydrothermal area is located on a still active and deep tectonic zone. The rhyolite and obisidian flows are strongly foliated and the top part is hydrothermally altered. The severe refolding of the rock bodies gives rise to peculiar foliation structures which are characterised by tension and laminar fractures.

2.2.1 Stratigraphy

As the work of Alula. (1990) and Woldu .(1994), explain in the area under investigation one finds various types of volcanic rock exposed which were the results of volcanism from Pliocene to Recent (Mohr 1987 and other). Several volcanoes were active contemporaneously as

evidenced by the interfiguring of their products. Most of the exposures are limited to river and road cuts covered by either reworked volcano clastic deposits or extensive ash flow units.

The lithological character of unit for the Boku area is summarised hereunder according to the suggested stratigraphic position from bottom to top.

The rocks of the Boku group are associated with a large central volcano and several smaller centres outcropping near Wagillo. The volcanic products connected with the activity of these centres, observed to extend as far as the Jogo ridge and fill all the depressions found in the western part of the study area .

These rocks are constituted by a base of acidic lava flow unit covered by a pyroclastic flow unit characterised by pumice fall deposits, ignimbrites and ash flow.

Older Acidic Lava Flows

Older acidic volcanics which occur as lava flows from the Boku ridge (south of Nazareth) in the study area. The flows mainly constitute white rhyolite unit which is often associated with obsidian layers. Occasional layers of pumice and ash have also been observed. Dues to alteration and also due to their small size phenocrysts are scarce in many rhyolites from different parts of the ridge. The thickness of the flows in this area is estimated to be more than 100 m. Flow structures like banding and folding are evident in these rhyolites.

Petrographic study of the representative samples from the rhyolitic flows of the Boku Ridge reveal that the rocks are generally scarcely porphyritic with glassy to micro crystalline (sometimes cryptocrystalline) felsic ground mass which occasionally contains microlites of alkali feldspar. Phenocrysts are mainly alkali feldspar , quartz and rare aegrine. Flow structures are also evident in some thin sections. No clear field evidence could be observed to ascertain the relative position and relation between other lithologic units in the area and acidic flows of Boku

ridge Woldu A. et al., (1994). However, data from Begazzi et al., (1981) indicate an absolute age of about 0.8my and younger for these flows. The older acidic flows at Boku are intensely dissected by major normal faults.

Pyroclastic Flow and Fall

The rocks of this group are exposed over wide areas at Wagillo, Boku, near Nazareth city dump, at Kimbibit river and in a quarry located along the Koka Nazareth road.

At Wagillo, this unit is constituted by 10m thick, weakly stratified, coarse, fine depleted pumice fall deposit. The pumice clasts are sub-angular and are interlayered with 1km thick grey well welded ignimbrite, patches of dark glass and grey, fine ash flow deposits.

Near Boku ridge, in a small quarry, a 5m thick very coarse pumice fall deposit carrying large lenses of obsidian occur.

At the Nazareth city dump, this unit is made up by a base of coarse angular, fine depleted pumice fall deposit carrying levels of grey and brown ash giving an overall appearance of weak stratification. On top of this section, separated by 20cm thick brown paleosol, 60cm,thick well-welded grey ignimbrite occur. Finally a whitish, 3-4cm thick scarcely welded coarse ignimbrite rich in pumice clasts and litnic fragments cap all the unit.

At Kimbibit river, rocks of this group cover a basalt unit of Dera-Nazareth group. This section starts with a base of 1.5m thick, black, fine grained, glassy ignimbrite followed by a total of 6m thick, brown to grey ash flows separated by thin horizons of paleosol.

The best outcrop of this unit is located in a quarry found along Kika-Nazareth road. The deposit is constituted almost entirely by weakly stratified coarse grained pumice fall containing layers of grey to brown fine grained ash flow deposits and centimetric levels of paleosol.

2.2.2 Observed Structural Features

Regarding the structural geology of the area, in the Boku and Wagillo area several remnants of caldera rims, evidenced by their curved outline and constituted by rhyolitic lava flow are present. The largest one, the Boku ridge is facing northeast and has 160-m height. Its flank is cut by north-south oriented faults forming a 1km wide graben along which strong hydrothermal activity occurs. Similar but less curved ridge is present in the Jogo area which is constituted by composite curved ridges facing west.

Cinder and spatter products of basaltic composition (scoria and scoraceous basalts) are abundantly distributed in the form of cones in the study area. These cones mainly occur Southeast and Southwest (around Wonji) of Nazareth town. They are preferentially distributed along north-Northeast oriented narrow zone, commonly known as the Wonji Fault Belt (Mohr, 1960). The cones are constructed around central vents, and show clear alignments along young fissures(faults).

The quarry of pumice fall deposit of the Boku group located along the city dump near Nazareth is affected by meso-scale normal faults whose orientation range from north-Northeast to east-Northeast direction. Alula et al., (1990).

3. SURFACE AND GROUND WATER HYDROLOGY

As Tamiru and Vernier (1997) pointed out the Ethiopian Rift Valley is characterised by high geothermal energy and hydrothermal activity attributed to its high thermal anomaly. A large number of thermal springs and fumaroles are associated with central acidic volcanoes, where younger fractures that postdate the volcanic activity discharge hydrothermal fluids. These fractures, in the central part of Ethiopian Rift are represented by the Wonji Fault Belt (Mohr, 1971; Di Paola, 1972), which tap thermal water and steam from the underlying geothermal reservoirs that are probably located near shallow magma chambers.

The studied area is located near the Boku Caldera which directly shows the presence of collapsed magma chamber underneath. The Pliocene ignimbrites and basalts are the important aquifers in the Ethiopian Rift Valley both from hydrological Tamiru (1993) and geothermal point of view Tesfaye (1982) Berhanu (1996) . The groundwater temperatures in these aquifers, for example in the Nazareth area with bore hole depth of 100 m., reaches 26 ^{0}C. In the nearby Debre Zeit area, the temperature of the groundwater within basaltic and ignimbritic aquifers at a depth of 140 m., is about 18 ^{0}C, which is a characteristic value for the normal ground water Tamiru and Vernier (1995).

The high temperature anomaly of groundwater in the Nazareth area could be attributed to the shallow location of high geothermal gradients that are due to repeated tectonic and volcanic activities. In the investigated area, the floor complex ignimbrites are extremely welded and intensively fractured, so that taking into consideration also their stratigraphic position, they are promising aquifers, where fracture permeability prevails on pore permeability.

running faults (fig 3). These faults, indeed, may feed vertical laminar fractures and tension fractures and act as a vertical pipeline. The foliation fractures (tension cracks and laminar fractures) increasing largely the vertical permeability rhyolite. The deep running recent faults are substantially inclined and curved to reach high thermal anomaly areas. The infiltrating water from South and South-western parts, mainly from the great alluvial terrain fed by Awash river, may recharge the high geothermal gradient areas. The minimum theoretical depth of the provenance of thermal water can be evaluated using the formula given by Celico (1986).

$$P = P_e + (T-T_a)\,G$$

where : P = minimum theoretical depth (m)

P_e = the thickness (m) of the rock which could be affected by external temperature;

T = temperature of thermal water (^{0}C);

T_a = temperature of infiltrating water, ^{0}C (equal to mean yearly air temperature minus 2 or 3 ^{0}C

G = geothermal gradient (m/ ^{0}c)

The geothermal gradient in the Ethiopian Rift Valley, as calculated from the temperature data of Birhanu G. (1993, 1996), is about 6m/ ^{0}c Tamiru A and A. Vernier. P_e is extremely variable, ranging from 15 to 17 m in the porous rocks, from 24 to 27 m in limestone, and from 35 to 39 in granites (Celico, 1986). Since rhyolites are the dominant lithology in the studied area, it is possible to say that volcanic rocks are more compacted than limestone, but less than granites, so that, for their massive nature they could transmit the effect of external temperature at a greater depth, which could be assumed to be closer to granites. Hence, for Boku rhyolites, the value of 35 m. is considered for P_e . T_a being = 15 ^{0}C and T = 78 ^{0}C, then the calculated value of P will be 413m. This value could also be considered as minimum depth of tapping fractures.

Since the steam temperature at the surface is undoubtedly higher than the condensed water, the expected value of P will also be high. In fact, other factors being constant, a value of 100 ^{0}C for T would give a value of 545 m for P. The steam and the thermal water (actually in small drops) may have the same aquifer. However, the steam may be partially transformed transformed into hot water by contact with shallow cold water.

3.2 Rain Fall

The main part of this work stems from information obtained from the work of Getahun K. of the EIGS(1987) hydrogeology of the Nazareth area. As explained by Getahun, Seventeen rainfall stations have been installed by the National Climatological Service and Valley Development Authority out of which 15 are in the middle Awash, 1 in the Zwai drainage basin at Abura and 1 in the upstream part of the Wabi Shebelle drainage basin. Those at Kola, Wonji, Metahara and Abura belong to class 1 where rainfall, temperature, relative humidity, wind speed, radiation and evaporation are recorded. That of Nazareth and Kulumsa belong to class 3 where rainfall and temperature are recorded.

A summary of 4 to 25 years of the mean monthly rainfall data is given in Table (3) from which the histogram of rainfall for selected station is drawn (fig 4)

According to the isohyetal map, climate in the area is governed by altitude variation of air temperature and precipitation occurs On the Minjar Shenkora high land where the altitude is greater than 2000 meters above mean sea level, annual rainfall varies from 900 to 1000 mm/year and gradually decreases eastward to 500 mm/year at Metahara in the rift which has an altitude of 955 meters above mean sea level. Within the rift, altitude decreases from Southwest to Northeast. In the same way the mean annual rainfall decreases from 700 mm/year in the Southwest to 500 mm/year at Methara located in the Southwest of the Main Ethiopian Rift.

From the main monthly rainfall data, the monthly rainfall coefficients are calculated for all station in the area, Table (4).

A month may be considered as rainy as soon as the monthly rainfall coefficient reaches 0.6 (60% of the rainfall module), and distinctly rainy when it exceeds 0.8. Extremely rainy months have a coefficient of more than 1, i.e., the rainfall exceeds the module value (Awash River basin vol. III; RAO, 1965).

According to the rainfall coefficients, three seasons are recognised: namely the Rainy, Dry and small rain seasons.

3.3 Evapotranspiration

Due to lack of sufficient data, it was not possible to determine exactly the evaporation and evapotranspiration of the studied area. But it is possible to estimate the evapotranspiration of the areas based on the results available for areas which have got similar climate patterns.

The main factor affecting evaporation is the total solar radiation. Evaporation measurements using a Colorado type pan taken by the National Climatological Service and the Valleys Development Authority for stations at Koka, Wonji, and Metahara. A summary of the mean monthly and annual evaporation values are given in Table(4).

The potential evapotranspiration for areas having temperatures below 26.5 ^{0}C are taken from Nomogram For the evaluation of standardised monthly potential evapotranspiration and for areas having temperatures exceeding 26.5 ^{0}C from a table by Thornthwaite. In table(4) it can be seen that except July, August and September, the potential evapotranspiration is greater than precipitation for most of the months but for Methara area the potential evapotranspiration is greater than precipitation for all the months.

Mean annual rainfall and mean annual evapotranspiration plots (Fig. 5) show that the towns of Koka, Wonji. According to Fig. (5) potential evapotranspiration and precipitation values would be equal at the altitude of 1800m above mean sea level.

TABLE 3 - MEAN MONTHLY RAINFALL

Station	Altitude in meters	No. of years of record	Jan.	Feb.	Mar.	Apr.	May	June	July	Aug.	Sept.	Oct	Nov.	Dec	TOTAL
Chefe Donsa	2400	7	18.8	22.4	53.3	46.7	93.5	106.1	283.8	265.9	106.7	7.7	0.5	2.1	967
Ejere	2245	6	15.0	15.1	54.4	59.9	67.0	86.9	228.4	219.4	113.3	1.5	2.8	8.2	929
Bolchi	1820	7	19.1	29.4	37.0	35.5	54.7	69.7	263.8	242.4	99.0	5.3	2.0	5.2	862
Bollo Gucrgie	2000		27.3	27.3	43.3	25.0	45.5	57.7	220.4	204.5	83.0	4.5	7.0	4.8	755.
Mojo	1870	7	15.6	27.7	56.8	53.3	62.7	116.1	263.0	186.1	114.7	11.5	2.0	2.0	911.
Koka H.E.L.P.A.	1592	22	14.2	21.6	42.8	50.6	40.0	62.5	197.9	170.6	93.5	21.9	5.7	8.5	729.
Bharet	1650	10	15.5	28.1	33.5	43.0	34.2	92.2	234.4	200.4	78.5	11.6	15.0	6.4	799.8
Welenchiti	1495	6	51.4	66.2	82.1	75.9	72.7	62.9	241.4	238.4	108.0	5.7	3.9	11.8	1020.4
Wonji	1540	25	10.0	20.6	51.0	63.9	48.6	74.1	201.9	198.0	104.7	28.7	6.3	7.7	816.3
Koleta	1600	7	15.1	16.8	60.8	57.0	75.7	91.3	178.8	151.2	142.8	20.2	4.6	1.9	816.2
Kulumsa	2200	7	37.1	32.9	98.5	51.2	79.1	91.1	130.5	143.4	111.5	15.1	6.2	6.5	803.1
Ibura	1648	7	13.2	34.2	54.9	54.9	41.1	63.9	130.1	92.7	94.1	12.0	0.77	5.8	597.7
Djersa	1845	7	17.6	31.2	64.4	45.3	65.2	87.1	196.6	172.4	123.4	10.2	2.0	4.9	826.8
Metahara	955	9	9.9	39.2	40.4	33.6	45.9	44.8	112.6	116.6	43.5	12.0	18.9	3.4	520.9
Awash	9916	106	22.1	39.8	54.5	43.4	29.4	34.2	123.4	154.3	49.6	11.1	16.4	3.9	582.1
Dire	1980	7	4.2	10.9	77.0	85.5	57.5	91.8	171.8	168.7	167.9	44.8	15.0	2.1	897.2
Gineh	1720	4	46.3	16.8	122.4	162.4	150.9	172.1	219.6	198.3	168.6	52.7	20.4	42.2	1872.7

3.4 Recharge and Discharge Processes

As indicated in the report of Getahun (1987), part of the high rainfall on the western and eastern highlands contribute varying amount of recharge to the groundwater depending on the soil, rock and topographic conditions in most regions, while the very large portion of the rainfall goes as quick run-off to the lowlands. On its way down the escarpment, some of the quick run-off is lost as recharge to the groundwater where streams cross fault zones.

Also Habteab and Melese (1987,unpublished) have explained, the surroundings of Boku mainly comprise of rhyolite and obsidian flows which are impermeable. Moreover, the domal structures and higher topography are favourable for quick run-off than infiltration or recharge and hence the area right at the vicinity of Boku steam centre is very poor for groundwater recharge.

On the other hand, the low land areas surrounding Boku are made up of up lacustrine deposits, alluvium and recent vesicular scoraceous basalt flows which are very permeable. In addition, faulting has created local grabens or depressions which are favourable for groundwater recharge and therefore, they are good recharge areas.

Generally speaking, the infiltrating water from the south and south-western part, mainly from the great alluvial terrain fed by Awash river, may reach the high geothermal gradient areas (Tamiru and Vernier, 1997). According to the hydrological model of the Boku fumarole, the area could correspond to the presence of deep floor complex ignimbrite aquifers with overlying refolded and fractured rhyolite lava domes. The rhyolite fracture pattern seems to increase the discharging area by tapping steam from the deep running faults.

3.5 Hydrothermal Manifestations

The typical evidence for the existence of geothermal fluids at depth is the presence of thermal springs, geysers, fumaroles, hot grounds, hydrothermal alternations, etc. As the technical

TABLE 4 – MEAN MONTHLY RAINFALL AND MEAN MONTHLY EVAPOTRANSPIRATION

Station	Elevation (m)		Jan.	Feb	Mar.	Apr.	May	June	July	Aug.	Sept.	Oct.	Nov.	Dec.	Mean Annua
Koka	1592	P	14.20	21.60	42.80	50.60	40.00	62.50	197.90	170.60	93.50	21.90	5.70	8.50	729.8
		ET	68.34	81.25	96.46	103.59	99.48	91.54	74.20	74.20	79.45	78.56	66.72	61.72	975.0
		Def	-54.16	-59.65	-53.66	-52.99	-59.48	-29.04	+123.7	+96.40	+14.05	-56.66	-61.02	-52.72	-245.
Wonji	1540	P	10	20.60	51.00	63.90	48.60	74.10	201.90	198.80	104.70	28.70	26.30	7.70	816.3
		ET	61.30	67.18	78.97	83.13	89.14	99.98	81.45	78.15	74.93	64.21	57.09	54.36	889.8
		Def	-51.3	-46.58	-27.97	-19.23	-40.54	-25.88	+120.45	+120.65	+28.775	-35.51	-50.79	-46.66	-73.5
Nazret	1620	P	15.50	28.10	33.50	43.00	34.20	99.20	234.40	200.40	78.50	11.60	15.00	6.40	799.8
		ET	63.92	77.13	82.66	89.91	87.97	85.53	72.32	74.20	78.78	70.75	62.46	52.70	898.4
		Def	-48.42	-49.03	-49.46	-46.91	-53.77	+13.67	+162.08	+126.20	+0.22820	-59.15	-47.46	-46.30	-98.6
Kulumsa	2200	PT	37.10	32.90	98.50	51.20	79.10	91.10	130.50	143.40	111.50	15.10	6.20	6.50	803.1
		ET	53.20	57.96	67.38	69.99	103.58	65.48	57.35	54.951	56.75	57.96	54.36	50.27	749.2
		Def	-16.10	-25.06	+31.12	-18.79	-24.48	+25.62	+73.15	+88.45	+54.75	-42.86	-48.16	-43.77	+53.9
Sire	1980	P	4.20	10.90	77.00	85.50	57.50	91.80	171.80	168.70	167.90	44.80	15.00	2.10	897.2
		ET	51.86	60.58	69.91	75.51	82.04	73.39	70.60	66.51	65.84	63.19	54.29	52.46	786.1
		Def	-47.66	-49.68	+7.09	+9.99	-24.54	+18.41	+101.20	+102.19	+102.06	-18.39	-39.39	-56.36	+11.0
Metahara	955	P	9.90	39.20	52.40	33.60	45.90	44.80	112.60	116.80	43.60	12.00	18.90	3.40	520.9
		ET	79.13	89.74	115.28	127.39	147.15	167.02	135.38	121.23	125.83	101.30	74.70	62.45	1346.
		Def	-69.23	-50.54	-74.88	-93.79	-101.25	+122.22	-22.78	-4.639	-82.23	-89.38	-55.80	-59.05	-739.
Awash	916	P	22.1	39.80	54.50	43.40	29.40	34.20	123.40	154.30	49.60	11.10	16.40	3.90	582.10
		ET	65.28	91.79	108.83	123.32	154.39	167.08	123.32	108.83	115.92	103.38	86.94	77.43	1322.8
		Def	-43.18	-51.99	-54.33	-79.92	-124.99	+132.88	+0.08	+45.47	+66.32	-92.28	-70.54	-69.53	-627.4

report from UNDP describes (1973) at Boku, the hydrothermally altered ground extends from 200 m along a fault thrown northeast. Near the south end of the altered zone weak fumaroles emerge on the scrap, temperature 74 ^{0}C. East from Boku at about 1km from the main steam centre, another zone of hydrothermal alternation up to 100 m wide, extends for 300 m along a south west downthrown fault within this area, there are several isolated patches of warm ground each of only a few square meters in area, with vapour escapes, Small huts have been erected and are being used as vapour baths. At both localities chalcedony and agate are common. Calcite, gypsum and oolitic silica are also reported.

4. GEOPHYSICAL RESULTS

4.1 Introduction

Electrical resistivity methods have been successfully applied in a number of geother
explorations to delineate subterranean hot water reservoir boundaries and sizes. The basis for
electrical resistivity surveying as applied to geothermal problems is the significant increase
electrical conductivity of rocks as they are saturated with thermal fluids. Thus, the objective of
method is to detect resistivity contrasts between the rocks in the geothermal zone and the roc
surrounding it.

The subsurface rock resistivity variations affect the electrical current flow and these in tu
affect the distribution of surface electrical potentials. Therefore, it is possible to obtain subsurfa
information from surface potential measurements. The commonly used resistivity survey method
to measure potential differences or gradients between two points using two current electrodes f
passing current into the ground. The usual current types introduced into the ground are direc
commuted or low frequency alternating currents. Potential differences are measured using nor
polarising electrodes.

The variation of resistivity with depth is studied by a progressive increase of the curre
electrode separation so that the effects of rocks at depth will be more significant. This method
known as Vertical Electrical Sounding (VES). Lateral resistivity variations are studied using
method of horizontal profiling for a fixed current electrode separation along a traverse line.

The resistivity value is determined from the relation developed using potential drop
current measures and the geometrical configuration of the electrodes. If the ground is homoge
and in a suitable location the resistivity is uniform, but in reality the ground is

inhomogeneous and the resistivity varies with the relative position of electrodes. The quantity then computed is known as the apparent resistivity (ρ_a).

4.1.1 The Concept of Apparent Resistivity

To understand the concept of apparent resistivity, it is important to discuss the flow of electric current in the ground and the distribution of potentials. The resistivity of a material is defined as the resistance in ohms between the opposite faces of a unit cube of the material. For a conducting cylinder of resistance R, length L and area of cross section A, the resistivity ρ is given by;

$$\rho = RA/L \qquad (4.1)$$

From ohm's law, the relationship of current, potential difference and resistance is given by:

$$dV = dRI \qquad (4.2)$$

substituting equation (4.2) in (4.1) ,

$$dV/dL = - \rho I/dA = - \rho I \qquad (4.3)$$

where: dV/dL = is the potential gradient (volt/ m)

i - is the current density (amp / m^2)

Considering a homogeneous and isotropic medium and a single current electrode on the surface, the current distribution is radial and uniform over a hemispherical shell developed by connective hemispheres of equipotential surfaces. With the centre at a current source C, fig (5) the current density at a distance r from a current source is given by

$$i = I/2\pi r \qquad (4.4)$$

where, $2\pi r$ = is the surface area of a hemispherical shell.

Thus, the potential gradient can be expressed by;

$$dV/dr = -\rho I = -\rho I/2\pi r^2 \qquad (4.5)$$

The potential at an arbitrary distance r relative to that at an infinity can be obtained by integrating equation (4.5) from r to infinity. Thus,

$$V_r = \int dV = -\int (\rho I/2\pi r^2)dr = \rho I/2\pi a \qquad (4.6)$$

Equation (4.6) is the basic equation of the electrical resistivity method to determine the resistivity of a homogeneous half space earth which can be given by

$$\rho = 2\pi a V/I \qquad (4.7)$$

or

$$\rho = 2\pi aR \qquad (4.8)$$

where R = earth resistance.

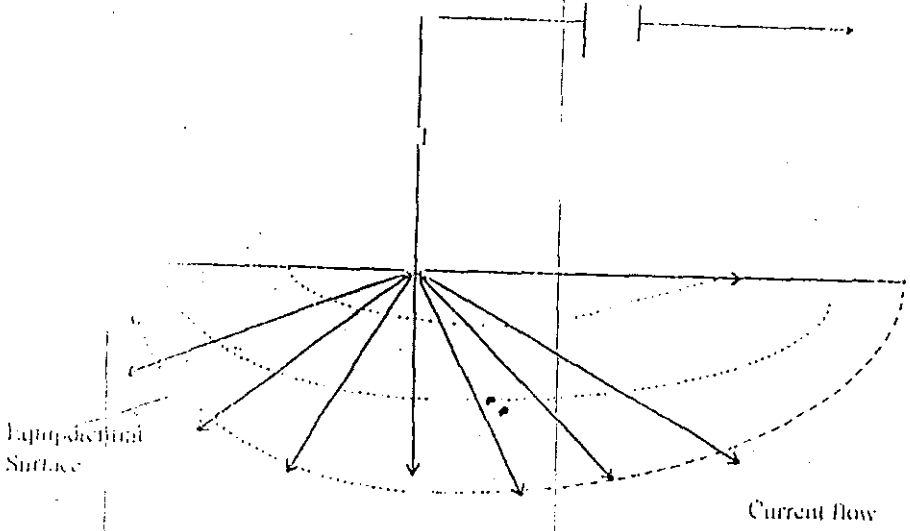

Fig (5.1) Current flow from a single surface electrode

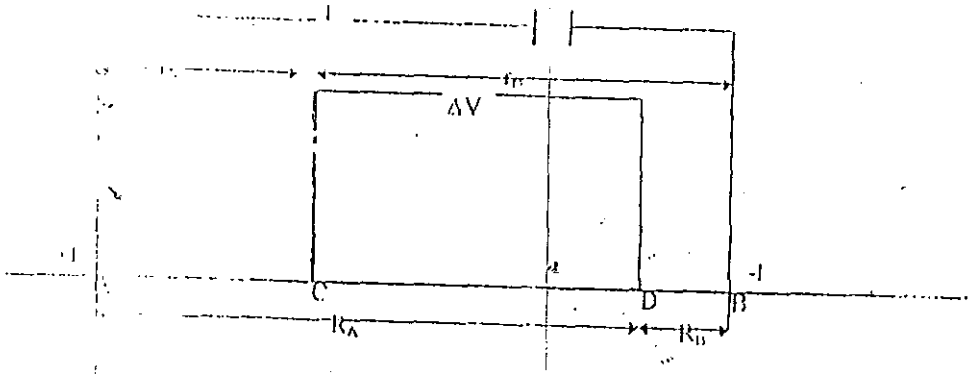

Fig (5.2) Generalized form of the electrode configuration used in resistivity measurements

If one considers a finite distance for the current sink using the general electrode configuration Fig (6) the potential of points at C and B, is thus,

$$V_M = V_A + V_B \qquad (4.9)$$

$$V_N = V_A + V_B \qquad (4.10)$$

where, V_A is potential contribution from current electrode A

V_B is potential contribution from current electrode B

Using equation (4.6)

$$V_M = \rho I/2\pi \ (1/r_A - 1/r_B)$$

$$V_N = \rho I/2\pi \ (1/R_A - 1/R_B) \qquad (4.11)$$

The potential difference between the inner electrodes M and N will be,

$$\Delta V = V_M - V_N = \rho I/2\pi \ [\ (1/r_A - 1/r_B\ ) - (1/R_A - 1/R_B) \qquad (4.12)$$

And the apparent resistivity is expressed as,

$$\rho_a = 2\pi\Delta V/I \ [\ (1/r_A - 1/r_B\ ) - (\ 1/R_A - 1/R_B)\ ] = KV/I \qquad (4.13)$$

where, K is a geometrical factor and expressed by,

$$K = 2\pi/\ (1/r_A - 1/r_B\ ) - (1/R_A - 1/R_B\ ) \qquad (4.14)$$

The resistivity calculated from equation (4.13) is constant and independent of electrode spacing and location for a homogeneous earth. But, for an inhomogeneous earth, resistivity varies and the computed value is called the apparent resistivity. Thus, equation (4.13) provides the basic

a single value of the current electrode spacing and the two values of the potential electrode spacing should be carried out at two or three consecutive values of the current electrode spacing. This procedure provides a reasonable amount of information on the effect of displacement of the potential electrodes on the measurements. The apparent resistivity for this configuration is given by:

$$\rho = K\ V/(I) \qquad (4.15)$$

4.2.2 Dipole-Dipole Configuration

In the dipole-dipole array, the electrodes are arranged in the sequence ABMN where M, N are not between A and B. In general, the lengths of AB and MN are made equal. By placing the electrode pairs in different orientations, it is possible to have various arrangements. The collinear dipole-dipole arrangement is shown in Fig. (7b)

In the collinear arrangement of dipole-dipole configuration the distance BM is selected to be either equal to MN or multiples of MN. ABMN are arranged sequentially along a line to be surveyed.

Since the array is symmetrical the point of measurement is generally considered to be at the centre of BM. When profiling at one depth of investigation is required the array, ABMN, is moved as a unit. It is possible to carry out profiling at several depths of investigation. In principle, the depth of penetration increases as the distance BM increases.

The main advantage of the collinear dipole-dipole technique is the reduced risk of EM coupling. The distance between the current source and the voltage receiver systems can be increased almost indefinitely, being subject to instrumental sensitivity and noise, where as the increase of electrode separations in the Schlumberger array is limited by cable lengths.

a)

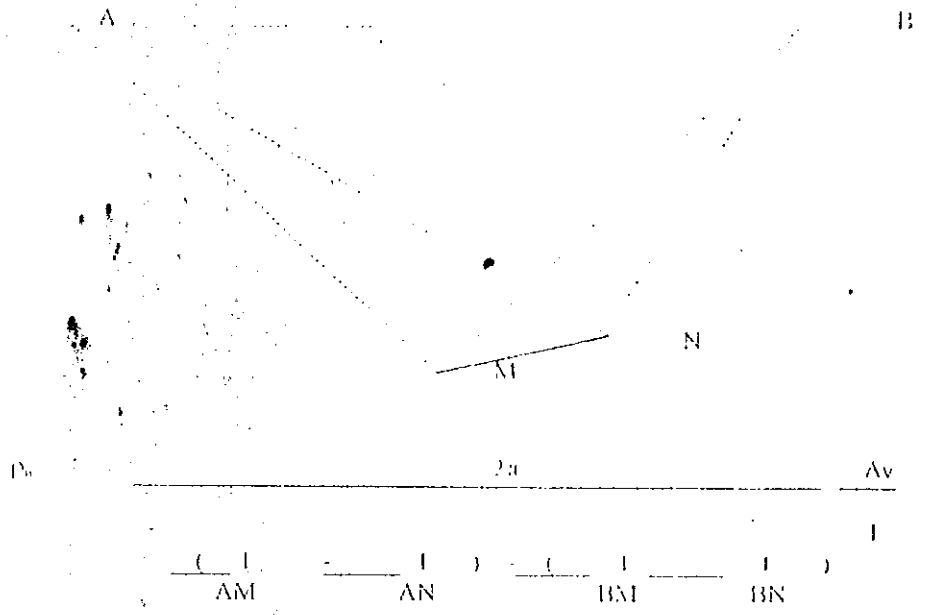

b)

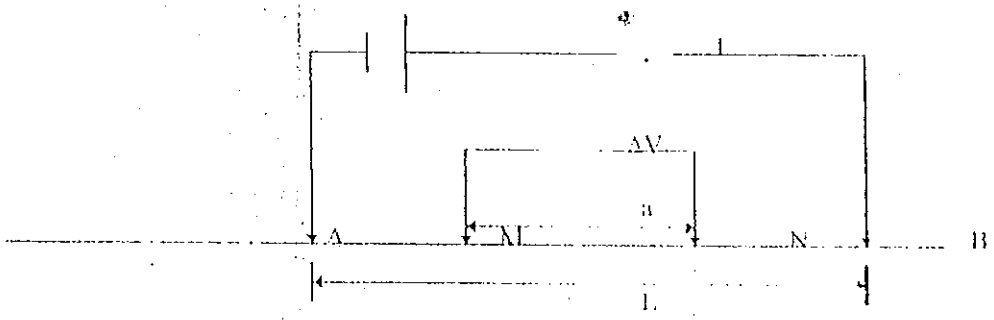

c)

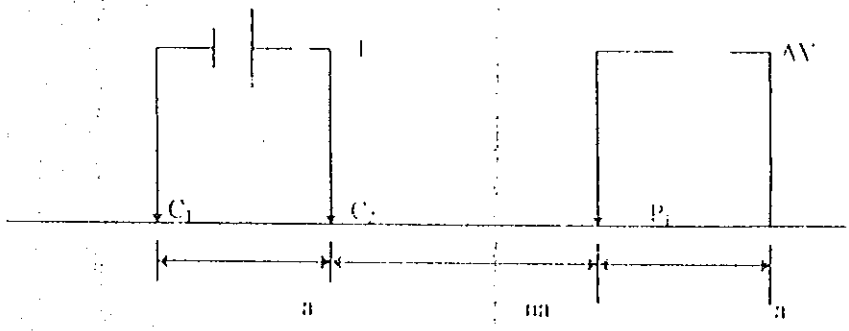

The apparent resistivity for this kind of arrangement system is given by :

$$\rho_a = n(n+1)(n+2)a\ (V/I) \qquad (4.16)$$

The collinear dipole-dipole electrode configuration is the most popular array for frequency induced by polarisation (IP) measurements. The configuration is used in geothermal exploration to delineate low resistivity zones related to a hydrothermal system. Topographic effects in resistivity surveys basically are caused by the use of flat earth geometric factors in the computation of apparent resistivity when the measurements are made over an irregular terrain.

Current lines diverge beneath a hill and converge beneath a valley. Therefore, the associated equipotential surfaces, which are normal to current lines also diverge under a hill, they produce lower potential differences relative to a flat earth and hence low apparent resistivities. In a valley, the converging equipotential surfaces results in high apparent resistivities. When a hill occurs between the transmitting and receiving dipoles, current focussing causes an apparent resistivity high. When there is a valley between the transmitting and receiving dipoles current dispersion produces an apparent resistivity low (Fox et al 1980).

Since the larger in values are associated with greater depths of investigation, the data can be arranged in a 2D pseudo-section plot which gives a simultaneous display of both horizontal and vertical variations in apparent resistivity. The conventional presentation places each measured value at the intersection of two 45-degree lines through the centres of the dipoles. Each horizontal data line is then associated with a special value of n and effective picture of vertical changes in apparent resistivity.

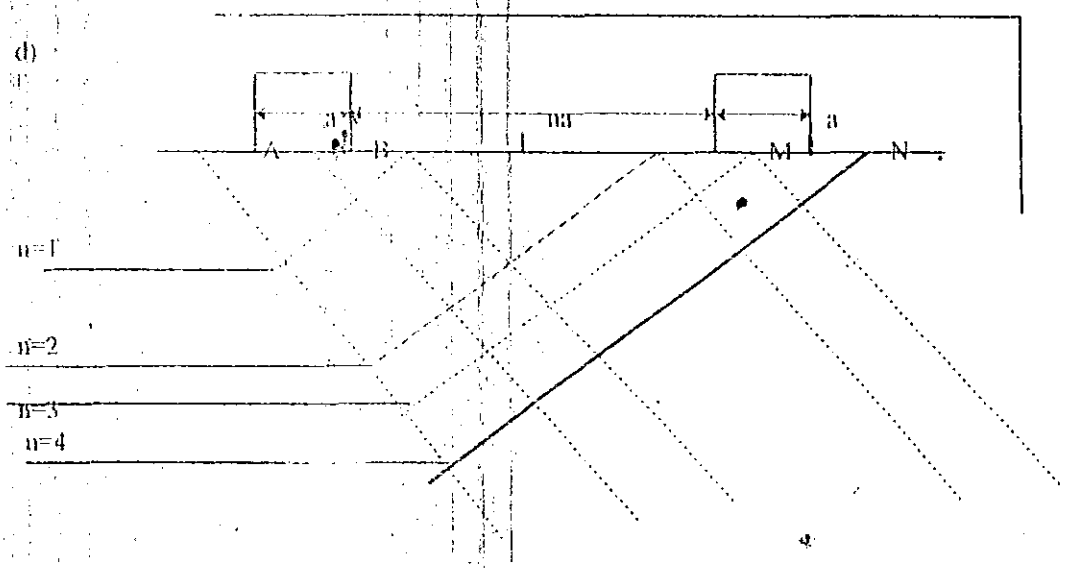

Fig (7)

a) A general four electrode configuration with a general formula of apparent resistivity
b) Schlumberger configuration
c) Dipole-dipole configuration
d) Conventional dipole-dipole psedosection plot

4.2.3 Electrode Spacing

For the field work carried out in the studied area, the electrode spacing for dipole-dipole (a) was 50m and the maximum innermost electrodes separation was also 50m. In the case of Schlumberger soundings the range of spacings (AB/2) was 1.5m - 500m and (MN/2) was 0.5m - 45m.

In the field, sounding data points were immediately plotted in a double log - log field book and decisions were made whether to repeat the measurement or not from the qualitative nature of the field curve by visual inspection.

The inter-electrode distances were already labelled on the eclectic cable which was wound around a reel which can rotate freely on an axle. Usually, sounding stations are along a profile mostly at an interval of 1km (depending on access) and spacings were along the profiles.

4.3 Sounding Data Reduction

The common initial procedure in vertical electrical sounding resistivity work is that apparent resistivity values are computed from field measurements of current (I), potential difference (V) and a geometric factor. The plotting is in such a way that the apparent resistivity values are plotted on a logarithmic scale as a function of electrode spacing which is half the electrode separation (AB/2). The apparent resistivity is plotted on the ordinate axis and the electrode spacing on the abscissa. The logarithmic scale results in the same movement of the curve for a given relative variation of the variables, regardless of their actual magnitudes.

The shape of a curve plotted in a logarithmic scale is preserved even when co-ordinates of each point along the curve are multiplied by arbitrary constants. This forms the basis for curve

matching. The scale also facilitates a comparison of the field curves with theoretical curves which are prepared in advance for a pre-determined succession of resistivity and spacing can be presented on a single graph.

In the Schlumberger configuration, the distance between the potential electrodes is increased as the distance between current electrodes is increased, otherwise the potential difference between M and N becomes too small to be measured for large separation of current electrodes. In principle, the depth range of the measurements increase as the current electrodes are displaced outward. As the ratio of the distance between the current electrodes to that between the potential electrodes gets large if it becomes necessary to increase the distance between the potential electrodes to obtain a sufficiently large voltage.

When the difference between the potential electrodes is changed, measurement at both the measuring electrode spacing should be made at least once, and usually two values for the same current electrode spacing. So the apparent resistivity values plotted from segmented resistivity curves corresponding to different potential electrode spacings. In most cases, the segments do not tie-in with each other for two reasons; firstly, the ratio of the measuring electrode spacing to current electrode spacing to current electrode spacing has a finite value (eccentricity of the electrode configuration).

Koefoed (1979) developed a correction for this failure of tie-in based on the linear filter method. He generalised the application of the method as the filter depends on two quantities only (samples of the input function), by means of two groups giving these quantities as functions of the eccentricity in the input function.

Mundry (1980) applied the eccentricity correction to Schlumberger sounding data in a similar procedure using linear and filter theory of Koefoed discussed above. A precise interpretation

of the sounding data requires a knowledge of the eccentricity effect, because a change in the geometry of the electrode array may change the form of the curve.

The second reason for the Schlumberger sounding curve not be tie-in between the segment is due to the occurrence of the near surface inhomogeneities in the ground. These inhomogeneities affect the current distribution pattern, and the relative change in the current density which they cause depends on the position of the measuring points with respect to the inhomogeneity. The relative error in the measured potential difference changes when the measuring electrodes are displayed. Kunetz (1996) defined the inhomogeneity effect as that caused by anything other than horizontal beds. Koefoed (1979) and Vnzjil (1985) have also considered lateral effects to be electrode effects.

In the present study, both corrections have been overcome by means of smoothing the field curve during the process of curve matching techniques.

4.4 The Principles of Equivalence and Suppression

In actual application of various interpretation methods to a particular field problem, limitations are set by maximum distance from the current source to which the electric field due to surface inhomogeneities. Furthermore, all measurements have finite accuracy. On account of all this causes, widely different resistivity distribution may lead to apparent resistivity curves which, although they are not identical, can not be distinguished in practice. This introduces ambiguity in the interpretation.

Mathematical formulation of two simple types of equivalence can be easily obtained. If we consider, for example, a relatively thin layer sandwiched between two layers whose resistivities are much larger than the sandwiched layer. Then the current flow in the earth will then tend to

concentrate into the middle layer (fig 9). The resistance of the elementary block of length , and cross section, h m, to such a current flow is

$$R = \rho\Delta l/h\Delta m \qquad (4.19)$$

and this will be unaltered if we increase ρ and at the same time increase in the same proportion. Thus, all such middle layers for which the ratio h/ρ is the same are electrically equivalent.

On the other hand, if the resistivity of the middle layer is much larger than that of the layers on either side of the middle layer, the electric current will tend to avoid it and take the shortest route to the lower layer. The lines of the current flow will be almost perpendicular to the layer Fig.(8). The resistance of the elementary block will be

$$R = \rho h/\Delta A \qquad (4.20)$$

where, A is the cross section. In this case, all layers for the product hρ is the same are electrically equivalent, so that, h, and P cannot be determined uniquely.

5. Magnetics Method

5.1 Introduction

The physical background of the magnetic method of geophysical prospecting is linked with the "potential " method, having its fundamental in the mathematical theory of the potential. The magnetic method even though is used as reconnaissance tool, there has been an increasing recognition of its value for evaluating prospective areas by virtue of the unique information it provides . Magnetic data are also used commonly to map thin magnetic sheets and /or contacts such as faults. An example of this is in petroleum exploration where magnetics is used to identify faults in the basement that may control the depositional history of the sedimentary basin. Magnetics have also been used in the magnetics anomalies associated with hydrothermal alteration which have been used in geothermal exploration, as has mapping of the magnetisation contrast at the Curie transition.

The fact that the characteristics of a rock which determines its magnetic effects, the intensity of magnetisation (dependent on its susceptibility) has both magnitude and direction, makes the magnetics method to be more complicated both in principle and practice. Also the magnetic force involves both attraction and repulsion and magnetic effects from rocks may be greatly influenced by small traces of certain minerals.

5.2 Principles and elementary Theory

Since magnetics method like gravity method is a potential field method its initial defining parameter is the magnetic force. The expression for magnetic force is obtained from coulombs law for magnetic poles and symbolically is given by:

$$F = (m_1 m_2/\mu r^2) r_1 \qquad (5.1)$$

where F- the magnetic force

m_1 & m_2 - the two magnetic poles

r_1- the unit vector

Amore practical quantity than the force is the strength of the magnetic field existing at a point in space, as a result of a pole of strength m located at a distance r from it. The magnetic field strength **H** is defined as the force on a unit pole :

$$\mathbf{H} = F/m' \qquad (5.2)$$

where m' is a fictitious pole at the point in space and is in effect the instrument of measurement.

Since magnetic poles always exist in pairs, the fundamental entity is the magnetic dipole, two poles of strength +m and -m separated by a distance l. Then the magnetic moment is defined as :

$$\mathbf{M} = m\, l\, \mathbf{r_1} \qquad (5.3)$$

M being a vector in the direction of the unit vector $\mathbf{r_1}$ extending from the negative pole towards the positive pole.

with their long dimensions across the external field. Paramagnetic and diamagnetic effects can only be observed in the presence of an external field.

The magnetic poles induced in a material by an external field H will produce a field of their own, H`, which is related to the intensity of magnetisation I by the formula

$$H`=4\Pi I \qquad (5.7)$$

The total magnetic flux inside the material, as measured in a narrow cavity having an axis perpendicular to the field, is called the magnetic induction B. This is the sum of the external and the internal fields and is proportional to the external strength in moderately magnetic materials, as shown by the relation

$$B=H+H'=H+4\Pi I=H+4\Pi KH$$

$$B=(1+4\Pi K)H=\mu H \qquad (5.8)$$

The proportionality constant $1+4\pi K$ is equivalent to the permeability μ. Thus equation (5.8) can be written as,

$$\mu=B/H=1+4\pi K \qquad (5.9)$$

The permeability is a measure of the modification by induction of the force of attraction or repulsion between two magnetic poles. Its magnitude depends on the magnetic properties of the medium in which the poles are immersed.

5.3. Magnetisation of Rocks:

Magnetic rocks have almost always acquired their polarisation from, the earth's field, the exceptions being the rare cases where the magnetisation has resulted from lightning. Often the polarisation is of the induced type, and its magnitude and direction are determined entirely by the magnitude and direction of the earth's field as it is today. When the earth's field changes, this kind of magnetisation changes accordingly. Other magnetic rocks display a remnant

magnetisation that is not related to the earth's present field but is governed instead by the field that existed when the rock was formed. If such a rock is igneous, its direction of magnetisation will be that of the earth's field at some time after it solidified and before it reached the curie point. This is called thermoremanent magnetisation. If the rock is sedimentary, any orientation of its magnetic grains during deposition, generally in quiet water, would have been an alignment with the field that existed when the deposition occurred. This is depositional remnant magnetisation.

The remnant magnetism of quickly cooled molten rocks (e.g., lava flows) is the record of the direction of the earth's field at the time of cooling, or solidification, due to the small grains of magnetite aligning with the direction of the earth's field. The study of the plate tectonics, sea floor spreading, and the geomagnetic -reversal time scale (COX^2).

5.3.1. The total Field and its components

Any magnetic field associated with a buried source is of course superimposed on that of the earth. The resultant field observed on the surface is a vector which has both magnitude and direction. Early instruments for measuring the field on landslide the magnetic balance were designed to read its horizontal or vertical components. Modern air borne and ship-towed instruments, on the other hand, measure the actual field, which is referred to as the total field, Interpretation of total fields, complex than that involving individual components, such as the vertical , which was the one generally recorded in most early measurement on land.

5.3.2. The Magnetic potential and Poisson's relation

The magnetic field has a potential , which is simply the work necessary to bring a unit magnetic pole from infinity to a point a distance r from another source of magnetic polarity of strength P. The magnetic potential U can be expressed by the relation;

$$U=1/\mu\ P/R \qquad (5.10)$$

The magnetic field is the spatial derivative of the potential. The direction of the field is determined by the direction associated with derivative. The X component of the field is simply du/dx, where x is in the direction of the resultant magnetic field.

The magnetic potential and hence the magnetic field strength associated with a magnetised body can be found at any point in terms of the gravitational potential by use of Poisson's relation. This is particularly valuable for predicting the magnetic defect of buried bodies. Magnetic fields from such bodies, even those with simple geometrical forms, are more difficult to derive directly than the corresponding gravitational fields. According to Poisson, the magnetic potential U can be expressed in the form

$$U=-I/\gamma\rho \, dV/Di \qquad (5.11)$$

where V= gravitational potential

i= direction of magnetic polarisation

I = magnetization or polarisation

ρ= density

γ= universal gravitational constant

The corresponding magnetic field component in any direction S is ,

$$H_S= -du/ds = I/\gamma\rho \, d(dv/di)/ds \qquad (5.12)$$

If H_z is polarised in the Z (vertical) direction, and if the horizontal component H_x of the magnetic field is desired, it can be obtained from the equation,

$$H_x =-du/dx =I/\gamma\rho \, d/dx(dv/dz) \qquad (5.13)$$

while the vertical component H_Z will be,

$$H_Z =-du/dz = I/\gamma\rho \, d^2v/dz^2 \qquad (5.14)$$

5.4. Magnetism of the Earth

Recently trends have developed in magnetic surveying toward analysing regional data to study large-scale geology as well as toward the use of more precision and detailing. With increased precision of field measurements, including precise geodetic control, adequate recognition of anomalies requires subtraction of the regional or background field . To determine what to subtract, familiarity with the earth's magnetism on a global scale is required. Fortunately , a large body of data of this kind has accumulated over the past century from magnetic observatories and field measurements.

The following are aspects of the earth's magnetism that have the greatest bearing on magnetic prospecting.

5.4.1.The Magnetic Elements and Their characteristics

At every point along the earth's surface, a magnetic needle free to orient itself in any direction around a pivot at its centre will assume a position in space determined by the direction of the earth's magnetic field F at that point. Normally this direction will be at an angle with north-south direction. Since measuring instruments conventionally installed in magnetic observatories respond only to the horizontal of vertical components of the actual field, it is customary to resolve X and Y projections) and its vertical component Z see Fig (9) . The angle which F makes with its horizontal component H is the inclination I, and the angle between H and X (which by convention points north) is the declination D.

The quantities X,Y,Z,D,I,H and F , known as the magnetic elements, are related as follows:

$$H = F \cos I$$

$$Z = F \sin I = H \tan I$$

$$X = H \cos D$$

$$Y = H \sin D$$

$$X^2 + Y^2 = H^2$$

$$X^2 + Y^2 + Z^2 = H^2 + Z^2 = F^2 \qquad (5.15)$$

All these relations are derivable from the diagram. The vertical plane through F and H is called the local magnetic meridian.

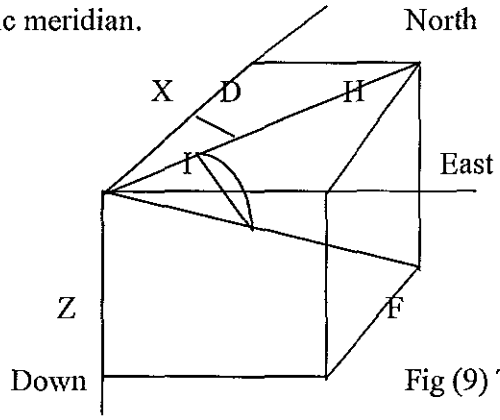

Fig (9) The Magnetic Elements

5.4.2. Variations of the Earth's Magnetic Field

From the study of information in navigation and measurements taken at magnetic observatories ., it was recognised that the earth's magnetic intensity changes its direction slowly and irregularly with time. The variations of the earth's magnetic intensity can be resolved into secular changes, solar diurnal changes, lunar-diurnal changes, and changes resulting from magnetic storms.

5.4.3. Secular Variation

Slow changes in the earth's field which take place progressively over decades or centuries are known as secular variations. /such changes are noted in all the magnetic elements at magnetic observatories everywhere in the world. The rates of change vary with time.

The projection of current rates of secular variation is not reliable means of determining past fields of predicting future ones. Paleomagnetic observations show that there have been variations as well as repeated reversals of the earth's field over geological time, the most recent

one taken place in a very short time. The mechanism for the reversals is not well understood, although most theories associate it with changes in the flow of electric currents within the earth which are induced by conducting material in the earth's core set into motion by convention.

5.4.4. Magnetic Storms

In addition to the predictable short-term variations in the earth's field, there are transient disturbances which by analogy with their meteorological counterparts are called magnetic storms. Such storms cause considerable disruption in magnetic prospecting operations. The oscillations that take place while they are going on are so rapid and unpredictable that it usually is not feasible to correct for them as with diurnal variations. Magnetic surveys must generally be discontinued during storms of any severity.

5.4.5 Corrections for Magnetic Variations

There are several ways of correcting magnetic data according to the various magnetic variations. For the secular variation of magnetic data a model which is known as the international Geomagnetic reference Field (IGRF) has been prepared from comparison of individual magnetic responses in different areas of magnetic observatories. So, it has become standard processing practice for magnetic survey that the applicable IGRF(updated to the time of the survey)is subtracted from the observed values of the total magnetic intensity.

The correction for the observed diurnal variation is more problematical, because the daily variation of the earth's magnetic field is highly variable and can not easily be approximated by a mathematical model. The necessary corrections are mostly attempted by the continuos observation of a base-station magnetometer located in or near the survey area. The measured magnetic field in the either through a direct subtraction of the two data sets of through the manual removal of corresponding anomalies from the observed survey data.

Since , variations in the magnetic field due to magnetic storms can be so rapid, unpredictable, and of such large amplitude, that normally discontinued under these conditions.

6 . DATA ACQUISITION AND INTERPRETATION

6.1 Electrical Method

6.1.1 Instruments Used and Data Acquisition

The instrument used for the present study in both the Schlumberger and dipole-dipole method are; an ac generator (Briggs-station) which has got a power out put of ( ); a TSQ-3 square wave transmitter which is connected to the ac generator by a three phase electrical cable and a receiver called IPR-8 which is connected to the potential electrodes.

In the present work, for the electrical sounding survey the field layout is divided into two profiles which are approximately parallel and separated by a distance of 500m. Six sounding stations are chosen with a spacing of approximately 1km for the first profile and four sounding stations are chosen on the second profile again their separation being 1km.

The current sent into the ground is read from the TSQ-3 square wave transmitter and IPR-8 receiver measures the resulting potential difference. The apparent resistivity value is calculated by using equation (4.9) and the measured apparent resistivity is plotted against AB/2 on a logarithmic paper right after each measurement to observe the curve trend on the field which is very helpful to correct out liars which are introduced by measurement errors and repeat observations if necessary before it is too late.

Nine VES stations are made using Schlumberger field array, six on the first profile with a spacing of about 1km and three on the second profile directed NE - SW direction. In this array a pulsed ac current is introduced into the ground through two outer

current electrodes A and B. The resulting potential is measured between two closely spaced inner electrodes M and N located at the centre of the sounding. Measurements are made at increasing current electrode spacing and the apparent resistivity is calculated using the relation,

$$\rho = K V/I \qquad (6.1)$$

Then the sounding curves are plotted using the values of apparent resistivity VS AB/2 of the Schlumberger expanding spread.

6.1.2 Interpretation

The aim of geophysical interpretation of sounding data is to determine the thickness and resistivity of different horizons from a study of the VES field curves and to use the se results to obtain a complete geological picture of the study area.

There are two types of interpretation, namely qualitative and quantitative interpretation. When the principles of equivalence and/or suppression do not allow quantitative interpretation, quantitative interpretation is carried out. Vertical electrical soundings are interpreted to express the results obtained from field measurements in terms of geological formations.

It is very important to find a relation for the electrical potential at the surface of the earth, in order to correlate the quantities that are measured and the parameters that define the resistivity stratification in the subsurface.

Two methods the image and Laplace solution methods have been developed to calculate the potential field in a layered medium.

The image solution was first proposed by Hummel (1932) and improved by a number of workers, Cagniard (1952); Koefoed (1932); Homilus (1961), and Orellena and Mooney (1966). The basis of this method lies in the assumption that the electric current behaves similarly to light rays in which case the electric current density and the light intensity decreases as the square of the distance from the origin increases. The method involves a single overburden of layers where the potential distribution due to a point source is determined in a medium by a plane boundary. Hence, the sum of the potentials due to a source at the surface and an infinite series of image sources or fictitious origins give the potential at a point on the surface.

The strength of each successive unique source is reduced by the reflection coefficient (K) between the layer boundaries. Then, the basic formula which determines the potential at any point on the surface is given by:

$$V(r) = (I\rho/2\pi)1/r \left[1 + \sum 2k^n r/\sqrt{(r^2+4n^2h^2)} \right] \qquad (6.2)$$

Where, r = the distance from the current sources to the measuring point

K = reflection coefficient $=(\rho_2 - \rho_1)/(\rho_2 + \rho_1)$, where ρ_1 and ρ_2 are resistivity values for two mediums

h = depth of the plane of the boundary

ρ_1 = resistivity of the first layer

This basic formula is extended to provide the potential distribution due to a four-electrode system where, at any potential electrode a potential due to two current sources is determined using equation (9).

Equation (4.15) can be used for developing the apparent resistivity expression for any four-electrode system using the potential field formulas for each array such as equation (4.12) for the Schlumberger configuration.

The formula provides the basic relation between ρ_a , ρ_1 ; the electrode spacing and the depth of the upper bed for any electrode system, so that the ratio ρ_a/ρ_1 is plotted against the ratio of electrode spacing over the depth of the upper bed.

The curves are plotted on BI-logarithmic scale which permits the preservation of the curve shape and a wide range of values to be presented on a single graph. Various master curves are prepared for different ratio of ρ_a /ρ_1 between $\pm \infty$; the most commonly used is the two layer curve. Interpretations using these standard curves are made by plotting field apparent resistivity curves on a transparent BI-logarithmic paper on the same scale of the master curve. The field curve is made to slide on the curves or a curve is interpolated between two adjacent curves.

The curves are moved parallel to the respective co-ordinate axis. The points where $\rho_a /\rho_1 = 1$ and $a/h = 1$ on the master sheet determines the values of ρ_1 and h on the field curve and ρ_2 is determined from the value of K.

In this work, two layer curves and auxiliary point methods were used in the interpretation procedures of this work.

In the second method, the potential field of any number of horizontal layers is obtained from the solution of Laplace equation for cylindrical co-ordinates. It has been derived by Stefanoscu and

Schlumberger (1930), and involves the determination of the potential at a point with respect to the resistivity of the upper must layer (ρ_1) and at distance r from a current source of length I.

It is defined by:

$$V = \rho_1 I/2\pi r \; [\; 1 + 2\int k(\lambda)\, j_0(\lambda_r)\, d\lambda \qquad (6.3)$$

where, V = the potential at a point on the surface

λ_r = a variable of interpolation

j_0 = Bessel function of zero order

$K(\lambda)$ = a Kernel function

$K(\lambda)$ is controlled by the thickness and resistivity of the underlying layers. The apparent resistivity for each configuration is defined with respect to ρ and r using equation (4.18) and the potential expressions for each configuration have been discussed in the previous sections. The main problem is the determination of the layer parameters, thickness and resistivity using the apparent resistivity expression.

6.1.2.1 Methods of Determining Layer Earth Parameters

The two popular interpretation methods which are in use today are the auxiliary point and the Pekeris - Koefoed method. A number of other methods are in practice nowadays which are trial-and-

error or optimisation approach. E.g. Ghosh (1971a, 1971b), Inman teal. (1973), Johnson (1975,1977).

6.1.2.2 The Auxiliary Point Method

It is Hummel (1932) who proposed the development of the auxiliary technique of sounding data interpretation. Later other scholars (workers) published theoretical resistivity sounding curves based on auxiliary point method. E.g. Ebert (1943), Cagniard (1952), Koefoed (1960), Homilius (1961) and Orellana and Mooney (1966).

The method is approximate and its accuracy decreases as the number of layers in the sounding curve increases.

In the auxiliary point method each of the branches of apparent resistivity curve is approximated by a two-layer theoretical apparent resistivity curve. This method is when the thickness of each successive layer is much greater than the combined thickness of all the overlying layers. The reduced sounding data are plotted on a double-logarithm transparent graph sheet preferably with modules of 62.5mm,with apparent resistivity on the ordinate and electrode spacing (AB/2) on the abscissa. Then, the plotted field curve is superimposed on the sets of two-layer master curves. The axes are kept parallel to the ordinate system of the master curve and the curve is shifted until a good fit is reached.

The co-ordinates of the origin of the master curves as traced from the field curve gives the values of P and h . The co-ordinates of the cross of these two-layer curves are considered to represent the thickness and the resistivity of a fictitious layer that represents the sequence of shallow formation. In this type of curve matching short segments of a resistivity sounding curve are selected

for interpretation using the theoretical curves for the single overburden, starting with the shorter spacing and working towards the longer spacings. As each portion of the curve is interpreted the layer comprising the interpreted portion of the sounding curves are lumped together to form a fictitious uniform layer with a lumped resistivity, ρ_1, and a lumped thickness, h_1 . This fictitious layer is then used in place of the surface layers when the next portion of the curve is analyses. This procedure is continuously used until the field resistivity curve is completely interpreted.

The auxiliary method of interpretation is a trial-and-error approach and a way of finding the first solution for subsequent optimisation of computer program.

In the present study sounding data were plotted on a double logarithm transparent graphs of modules 62.5mm. Orellana and Mooney (1966), two layer theoretical curves of 62.5mm modules with auxiliary curves (A,Q,H,K) were used for interpretation of the sounding curves. The model parameters (`true' resistivities and thicknesses) were used as initial model parameters in the optimisation method of interpretation. The 1-D resistivity model curves of sounding data of 10 stations, produced by using this method on the computer are presenter here.

Then the sounding curves are plotted using the values of apparent resistivity VS AB/2 of the Schlumberger expanding spread.

6.2 Magnetics Method

6.2.1. Instrument used and Data Acquisition

The instrument used in the present study is the integrated geophysical system (IGS2) geophysical equipment. The instrument measures the total magnetic field intensity and a digital display of the value is recorded. The survey has been carried out along three profiles, two of them, which are along the same line of the electrical resistivity and the gravity survey.

6.2.2. Interpretation of Magnetic Data

Since the lows of potential theory are fundamental in magnetics method, the techniques employed for interpreting magnetic data have many similarities to most of gravity data interpretation.

There are two ways of interpreting magnetic data. These are the quantitative and qualitative interpretation methods.

A large amount of the effort put into interpreting data obtained in magnetic exploration might go no further than a qualitative evaluation of magnetic maps of profiles. The presence or absence of a fault or an intrusive body may be of much more important than its shape or its depth of burial, neither of which can be uniquely determined from magnetic data any way. In many magnetic surveys, the objective is to describe the boundary between sedimentary basins and surrounding areas where the basement is shallow.

Such information can often be obtained by visual inspection of a magnetic map. A basin is characterised by smooth contours and low magnetic relief, while the surrounding platform area shows steep gradients and high relief in the magnetic contours. Often a well-defined boundary between zones with appreciably different degrees of magnetic relief can indicate the presence of a major basement fault.

7.0 RESULTS AND DISCUSSION

7.1 Geoelectrical Sections

1. Profile 1

In the survey area, profile 1 consists of VES numbers 1-6. According to the VES data along the first profile, the geoelctrical sections of this profile has a five layered earth structure except at VES 3 which has a three layered earth structure. The analysis of the geoelectric and psedosections have provided useful information regarding the thickness and depth of layers. Fig (11).

The topmost layer along this profile at VES 1,2 and 3 is very thin whose thickness varies from 1.6m to 2m. The resistivity of this layer varies from 50Ω.m to 66Ω.m. This is a signature of very thin layer of alluvial cover.

The underlying second layer at VES 1,2 and 3 is described by range of resistivity 15Ω.m to 102Ω.m. Here a very conductive layer is observed at VES 2 and a very high resistive layer is observed at VES 3. The depth of this layer extends up to 4.7m from the surface. In this layer the very low resistive zone at VES 3can be an indication of weathered basalt or medium grained sand which is saturated.

The third geoelectric layer is characterised by a relative low resistive value at VES2 and 3whose value is 25Ω.m and 24Ω.m respectively and a high resistive value of 95Ω.m at VES1. This layer can be interpreted as a highly weathered and decomposed rock mass. Its depth ranges from 8m to 16m from the surface.

The fourth geoelectric layer is characterised by a relatively medium resistivity value of 32Ω.m and 85Ω.m at VES 1 AND 3. Here layer 4is missing at VES2 and this might be an indication of a fault zone at VES 2. The depth of this layer extends to 44m from the surface.

The fifth geoelectric layer at VES1 and 3 shows a resistivity value of 52Ω.m at VES3 and 702Ω.m at VES 1.Here the high resistivity value at VES1 can be interpreted ignimbrites. Again here the fifth layer is missing at VES 2.

VES 4 has 4 layers .the first two layers are very thin and layer 1 has a resistivity value of 27Ω.m and a thickness of o.4m and layer 2 has 94Ω.m and a thickness of 0.2m. Here the top can be associated with a weathered rock mass. The third layer at VES4 is a very low resistive layer and this can be associated with the hydrothermally altered zone which has got a high conductance. Then the forth layer is a very high resistive layer and this can be interpreted as a floor complex ignimbrites acquifer. The resistivity value of this layer corresponds to a value of 880Ω.m.

VES5 is located near to the fumarole site of the Boku thermal centre. As the geoelectric section shows it has a four layered earth structure. The top layer is very thin and has a resistivity value of 233Ω.m. Since this value is very high the top layer can be interpreted as rhyolite lava domes as this is highly resistive. Its thickness is 0.8m and its resistivity value is 52Ω.m. The third layer has a relatively low resistivity value of 40 Ω.m and its thickness 52-m. As we can see here a very thick rock mass is observed. Then the forth layer has a relatively high resistivity value of 93Ω.m.

VES6 has a five layered earth structure. The top layer is resistive and it has a value of 78Ω.m. Its thickness is 0.9m which is very thin. It can be associated with the rhyolitic lava

domes. Then a very low resistive zone is observed in the second layer which has got a value of 14Ω.m. This can be associated with the hydrothermally altered ground or rock mass. Its thickness is 20 m. The fourth layer is relatively resistive and has a value of 73Ω.m and it is very thick having a thickness of 49 m. The last layer is actually a highly resistive layer and it can be associated with the floor complex ignimbrites. It has got a resistivity value of 184Ω.m.

From the geoelectric section of VES 5 and 6 it is possible to infer that the area around VES 5 can have a fractured zone due to the variation of resistivity between VES 5 and 6.

2. Profile 2

The second profile is located at a distance of approximately 500-m north of the first profile. The second profile consists of VES 7,8 and 9. For the second profile also geoelectric section was constructed and the result is analysed. Fig (12).

The second profile at VES7 has a seven layered earth structure. The top layer is very thin and has a thickness of 0.9m and its resistivity value is 62Ω.m. The second layer and the third layer are a little bit thick and have a value of 2-m thickness. Their resistivity value ranges from 40Ω.m for the second layer to 82Ω.m at the third layer . Then the fourth layer has a resistivity value of 39Ω.m and a thickness of 3 m. The fifth layer is relatively high resistive layer and has a value of 190Ω.m and its thickness is 32 m and this can be associated with the hydrothermally altered zone having a high conductance value. Its thickness is 7 m. The basement layer is very high resistive layer and has a value of 984Ω.m. This actually can be interpreted as the rhyolitic lava domes since lavas have a very high resistive value.

VES 8 along the second profile has a three layered earth structure. The top layer is a resistive layer having a resistivity value of 90Ω.m and a thickness of 0.8 m and the second layer

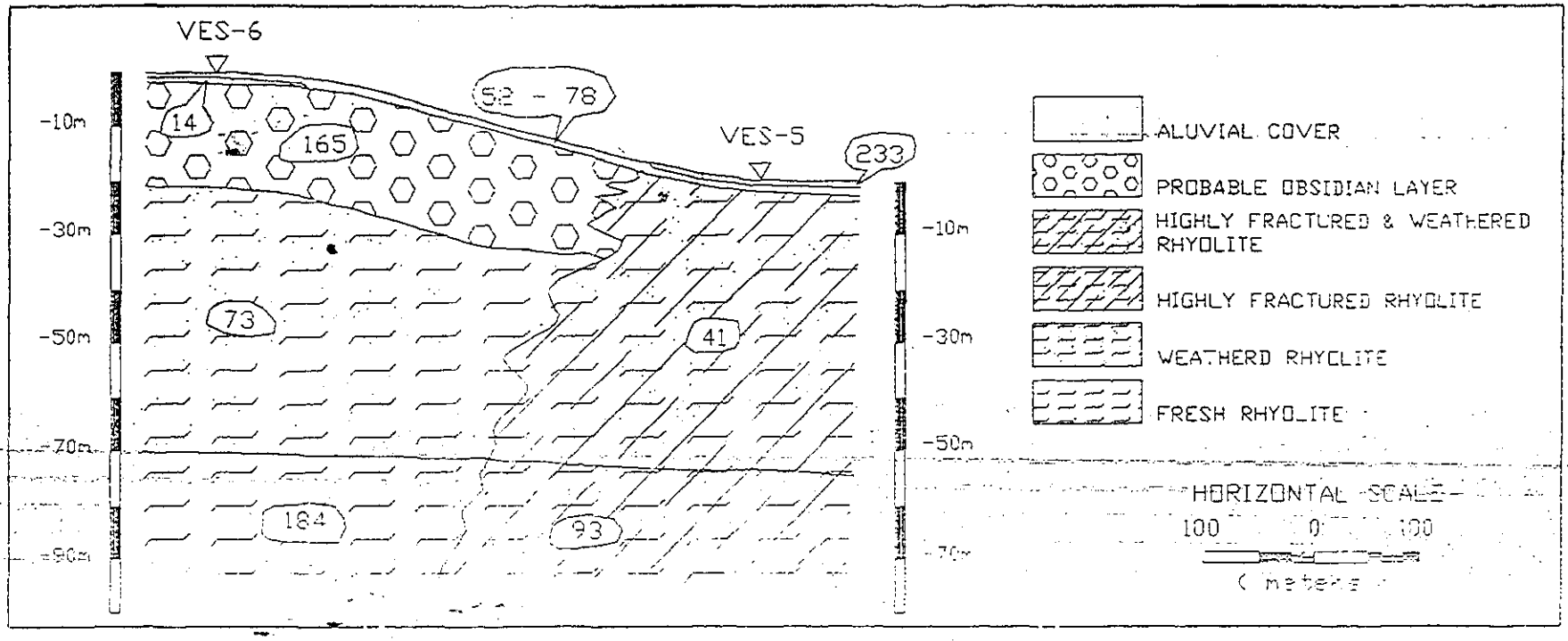

FIG.11b GEOELECTRIC SECTION OF BOKU THERMAL AREA, PROFILE ONE

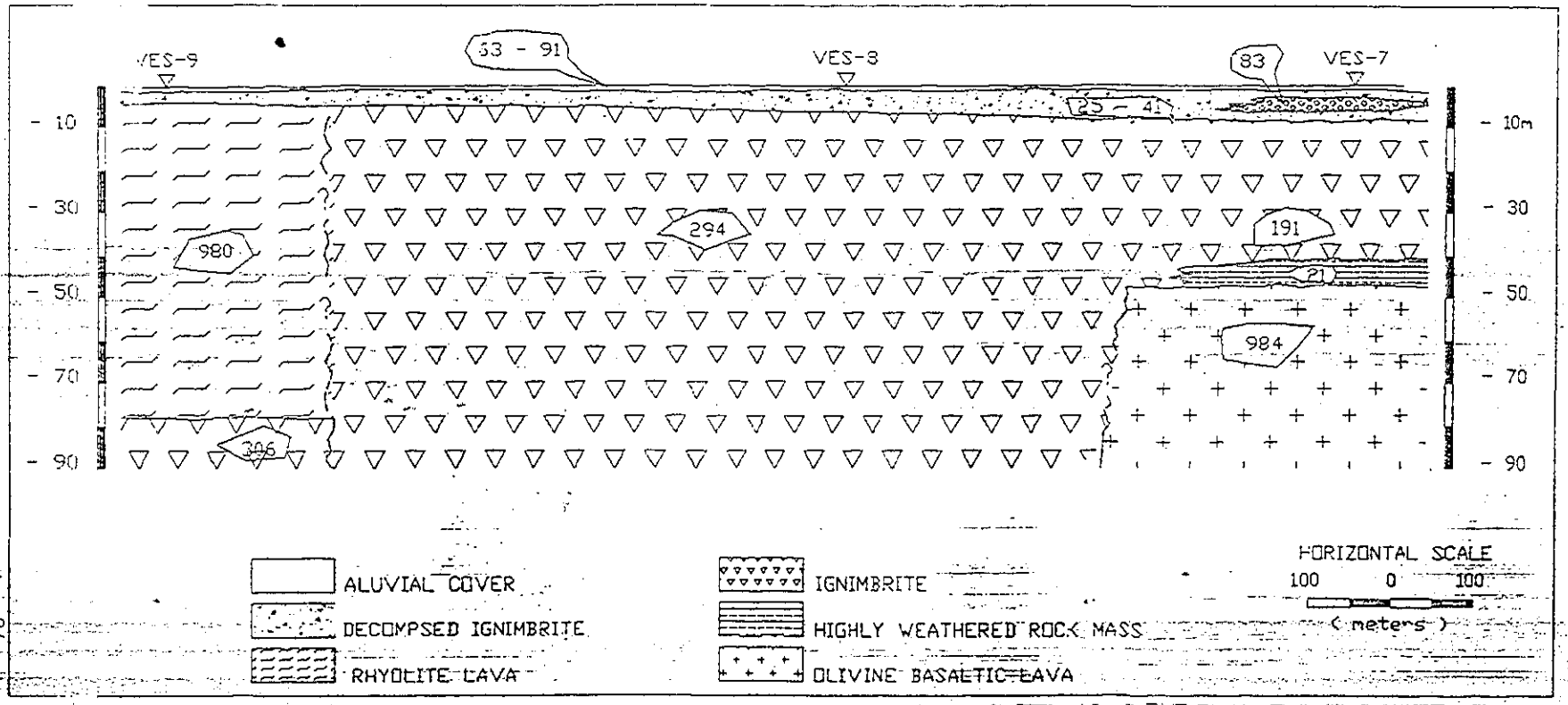

FIG.12 GEOELECTRICAL SECTION OF BOKU THERMAL AREA, PROFILE TWO

has a relatively low resistivity value of 24Ω.m. The third layer has a very high resistivity value of 294Ω.m and it is not actually possible to say this layer as a basement layer of VES 7.

Along VES 7,8 and 9 within the thick layers there are small lenses which has got resistive value ranging from small to moderate value and the presence of these lenses may affect the general resistivity trend of the Geoelectrical section.

7.2 Profiling Psedosection

A dipole-dipole profiling survey has been carried out only along the first profile and psedosections are constructed as shown Fig(13a,13b,13c).

On the first segment of the profiling psedosection a relatively high resistive is observed at the location of VES 1 and VESS 3 where as a very low resistive zone is observed around VES2. As we can see from the psedosection a certain geological structure is expected at the position of VES 2 which can be attributed as a lithological contact zone. This is because of the spatter cones which are located near VES1 and VES 3.The high resistive value at VES1and VES 3 might indicate the fact that the extension of these spatter cones are bounding the middle low resistive zone which is located at VES2.

The dipole-dipole psedoscetion along VES4 shows generally a high resistive lateral variation of the area. Along VES 5 there is a very low resistive zone from which we can guess that this is a sign of the hydrothermally altered zone. Here also relatively high resistive lateral variation is observed.

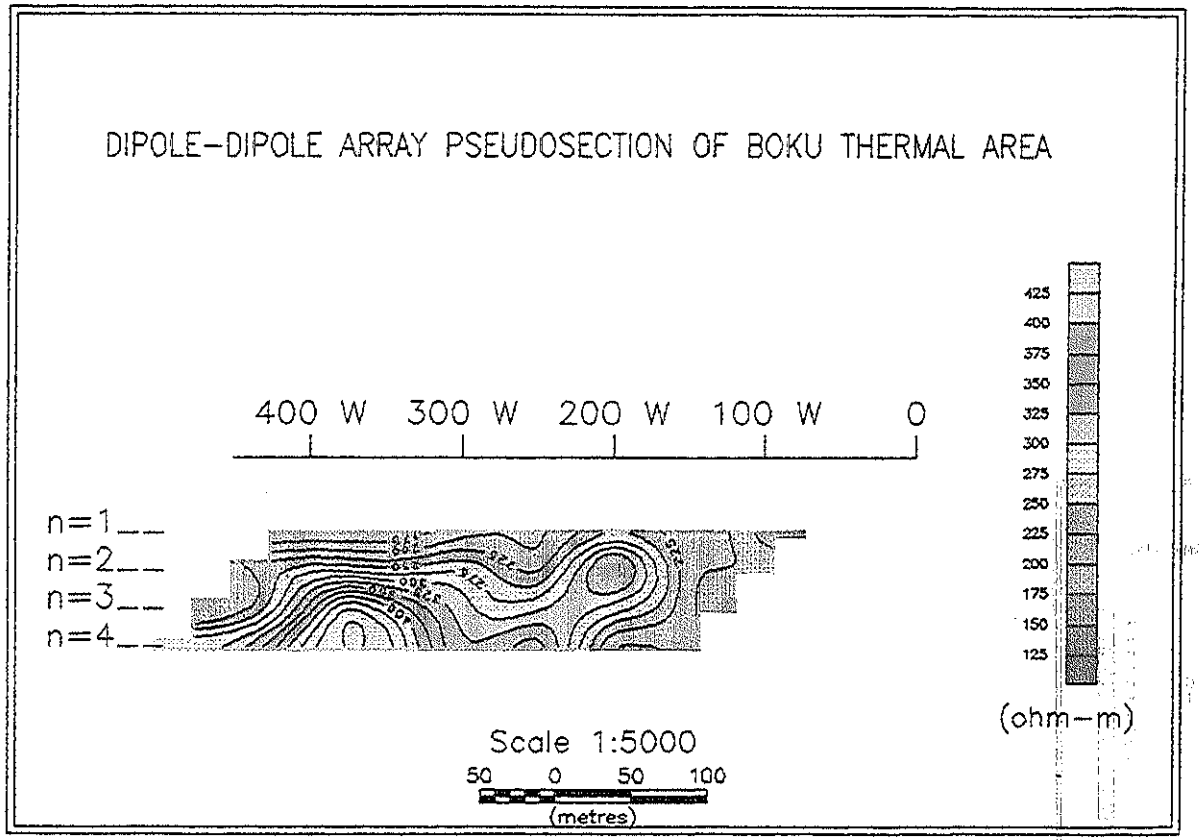

FIG. 13b PROFILE ONE, SEGMENT TWO

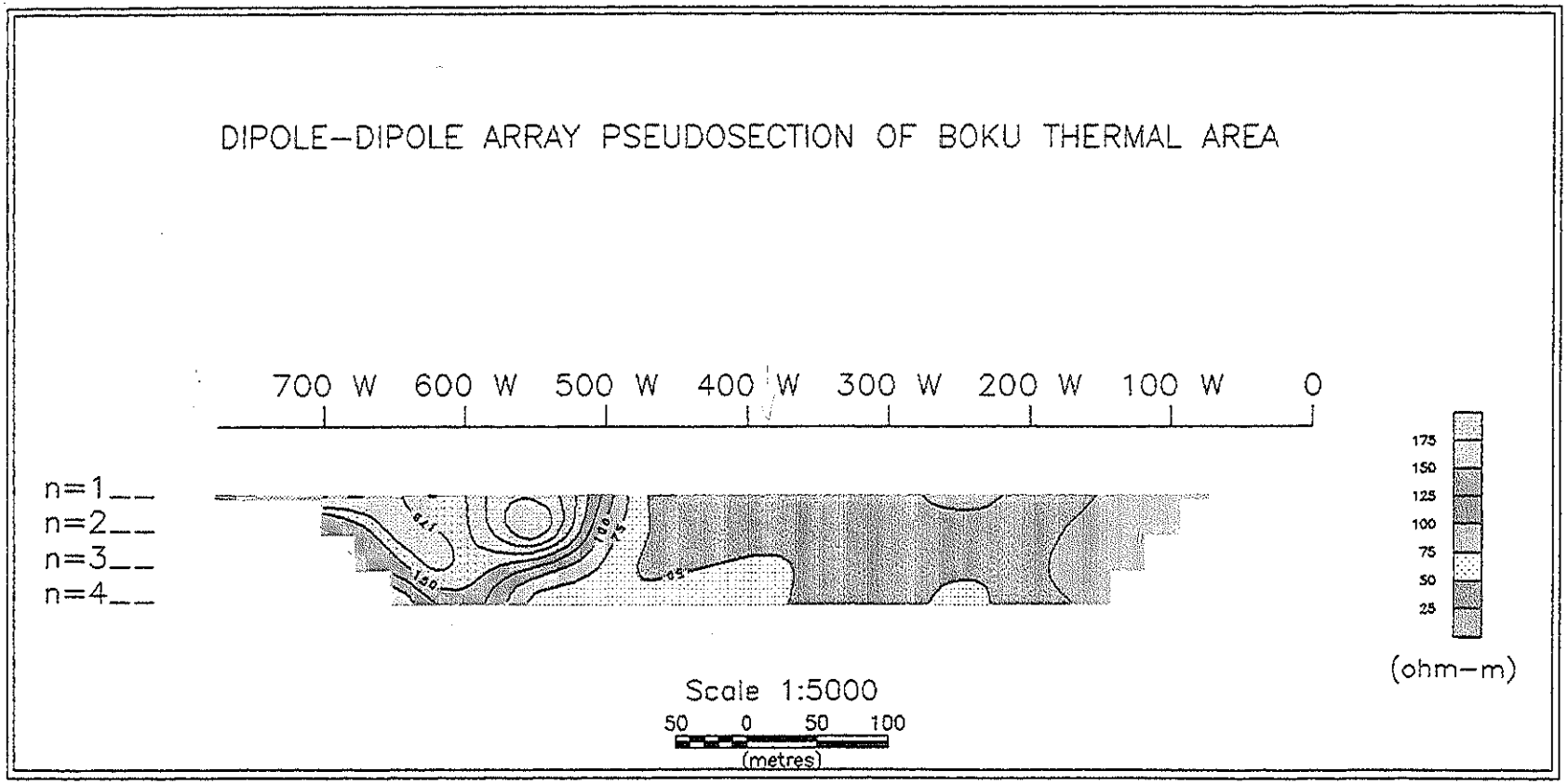

FIG. 13c PROFILE ONE, SEGMENT THREE

82

7.3 Magnetic profile

The magnetic survey has been carried out along three profiles where two of them are along the same line of the sounding survey. A qualitative interpretation has been carried out.

The first profile of the magnetics survey shows a very low magnetic anomaly around the position of VES1 Fig(14a).Also a very low magnetic anomaly has been observed at the position of VES5. Here we can see that a sharp disturbance is observed on the magnetic profile which can be associated with the structural features on the area Fig (14b). Again a very low magnetic anomaly is observed at the position of VES 6 which can also be associated with the structural feature of the area Fig (14c).

Profile two of the magnetics survey has also shown a very low magnetic anomaly along the parallel line of the location of VES 2 and VES6. Here disturbance of the magnetic anomaly is observed near the location of VES 2 Fig (14d).

The third profile of the magnetics survey has been carried out along VES 7,8 and 9.Here an erratic change of the profile is observed at the position of VES7 and VES9 Fig (14e).

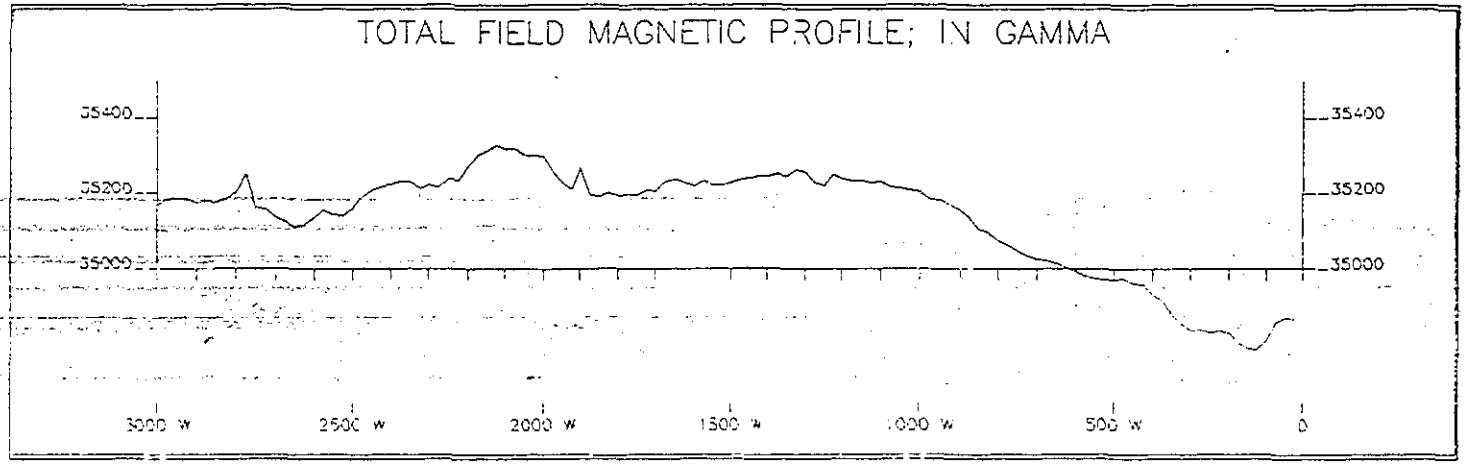

FIG. 11a PROFILE ONE

84

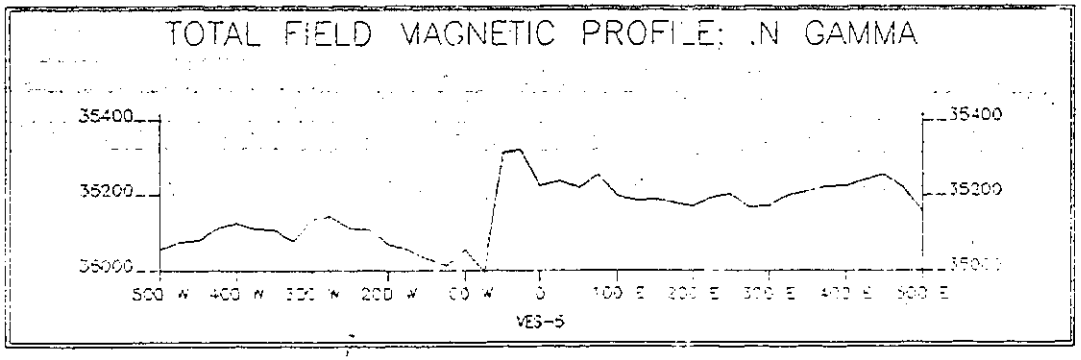

FIG. 145 PROFILE THROUGH VES-5

98

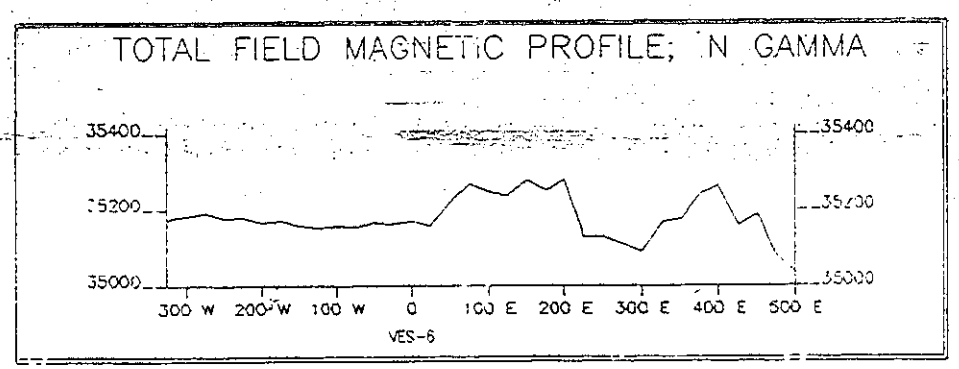

FIG.14C PROFILE THROUGH VES-6

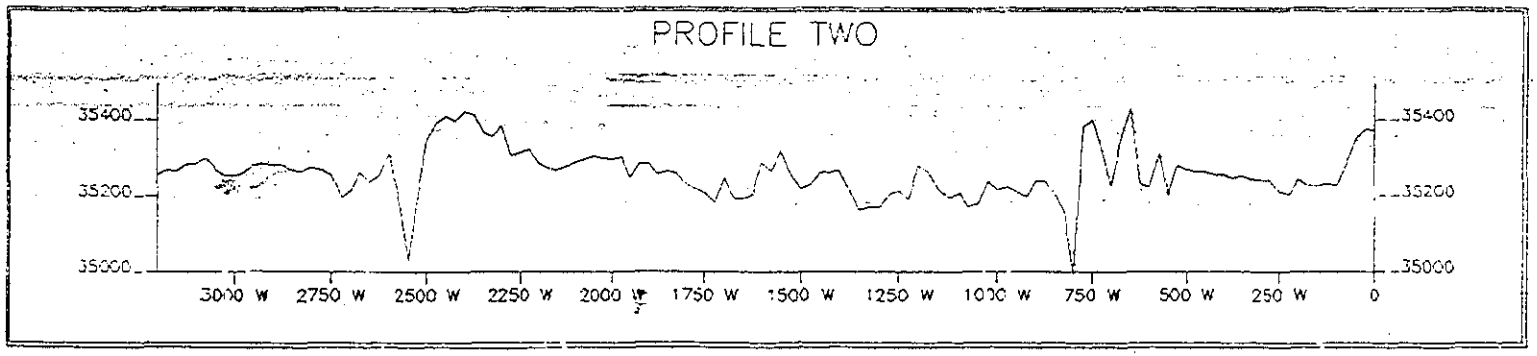

FIG. 14 d PROFILE TWO

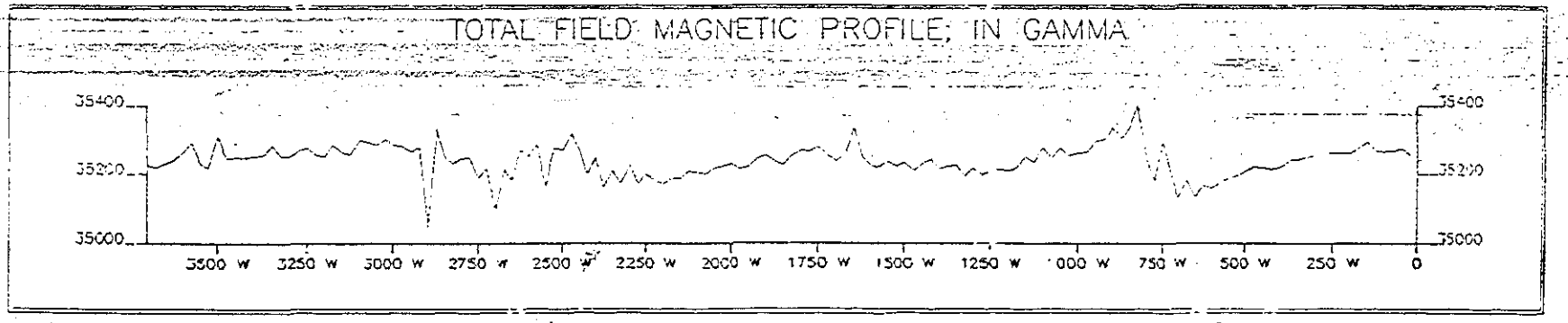

FIG. 14e PROFILE THREE

8.CONCLUSIONS AND RECOMMENDATIONS

Even though a detail geophysical survey is very important in the are specially seismic and gravity methods, all the available data collected and described in the present study indicate that the Boku thermal area has all the necessary characteristics for the existence of an exploitable geothermal potential.

The VES and profiling data it is possible to see that the western part of the survey area especially near to the fumarole site has shown a good structural features such as fractures and deep faults. Apart from that lithological contact zone is observed around the location of VES 1 -3 of the study area which includes. Profile two of the study area which includes VES 7,8 and 9 have shown an interesting feature characterised by a very low resistive zone for the large electrode separation. At depths of about 50 m around VES 7 and at a depth of 80 m around VES 9 it is possible to observe a very high conductance region which can be associated with the thermal water bearing structures.

The magnetics data has also shown a qualitative picture especially around the location of VES 1,2 and VES5,6. Here it is possible to see that a certain structural feature is expected. Regarding the conceptual model of the area, even though sufficient information is not available from the collected data the geophysical surveys have indicated a certain agreement with the proposed model. For instance, in the conceptual model it is indicated that the area is characterised by refolded and fractured rhyolite lava domes. This is in a good agreement with the VES data. For the minimum depth of the provenance of thermal water in the area, the VES results has shown that low resistive zones are observed at a depth of about 50 - 70 meters range..This showes that the low resistive zones are at shallow depth in contrast with the conceptual model of Tamiru & Venier. Actually to get a

clear picture for the hydrothermal activity of the area the present conclusions must be considered as a preliminary because for a complete understanding of the geothermal system in the study area, the following detailed investigations are needed:

1. A detailed geological survey is very important specially detailed lithologic & structural mapping , hydrochemistry , trace techniques isotopes along with geophysics (deep penetration) and also stratigraphic correlations of the area are very important.

2 . The VES survey must be carried out with the separation of the VES points very near to each other in order to get a better picture of the geoelctrical sections.

3. In order to get information about the deep geological structures of the area VES electrode separation possibly > 500 m.

4.Since the area is topographically inconvenient to carry out a gravity and seismic survey. Especially the gravity data will give a better structural feature of the area.

5. To overcome the lack of information regarding the geological settings of the area, boreholes are very important especially near to the fumarole site.

REFERENCES

Abiy, H., 1989 Gravity and Electrical resistivity sounding applied in Geothermal Exploration in the northern part of the Main Ethiopian Rift, MSc. thesis, University of Leicester.

Alula, D., 1990. Neotectonics of Nazareth-Dera area. M. sc. Thesis. AAU, Addis Ababa.

Alula, D, Bocaletti, M., Getaneh A, Mazzuoli, R. and Tortorici, L. ,1992. Geological Map of the Nazareth -Dera Region (Main Ethiopian Rift) 1:50,000 Cartography SELCA, Florence.

Befekadu, O., 1989. The application of Gravity and Electrical Resistivity Surveys to Geothermal Exploration in The Main Ethiopian Rift, MSc. thesis , University of Leicester.

Berhanu, G., 1993. Aluto-Langano Geothermal field, Ethiopian Rift Valley: physical characteristics and the effects of gas on well performance . Geothermics 22.

Berhanu, G.,1996. The origin of high bicarbonate and fluoride concentrations in waters of The Main Ethiopian Rift Valley, East African Rift System . Jour. Africa. Earth. Scien. 22

Bigazzi G. , Bonadonna F.P. , Di Paola G.M., & Giuliani A. (1981) . new K-Ar and Fission track ages of the last volcanotectonic phase in the Ethiopia Rift valley(Tullu Moy Area) proceedings of the first international symposium on crustal movements in Africa .Wassef A.M . , edt . ,

Cagniard, L., 1952. La Prospection Geophysique des eaux Sousterraines. In: Colloquue d'Ankara sur. 1' Hydrologie de la zone arid , UNESCO.

Celico,P.1986. Prospezioni Idrogeologiche. Liguori Editore, Napoli, Italy.

Combs,J., and Muffler, L.J.P., 1973. 'Exploration for geothermal resources.' In geothermal systems : Principles and case Histories . 1981. John Wiley & Sons Ltd.

Di Paola, G.M., 1972. The Ethiopian Rift Valley (Beween $7^0$00'and 8^0 40'lat. North).Bull. Volcanol 36.

Dobrin, M.B., and Savit,c.h., 1988. Introduction to Geophysical Prospecting, McGraw Hill Inc. Singapore.

Exert, A.,1943. Grundlagen Zur Auswertung geodekrischer tiefen messungen. Beitr. Angew. Geophys. Vol. 10.

Fox,r.c., Hohmann,G.W., Killpack,T.J., and Rijo,L.,1980. Topographic effects in resistivity and induced polarization Surveys. Geophys. Vol. 45.

Gidey, W.,et al. 1990. Geology, Geochronology and rift basin development in the central sector of the Main Ethiopian Rift. Bull. Geol. Soc. America, Vol. 102, 439-458.

Getahun, K., 1987. Hydrogeology of Nazareth Area, NC 37 - 15,Note 268,Addis Ababa.

Gezahegne, Y., 1980. Geothermal study in northwest lake Abaya area. M. Sc. Thesis. AAU, Addis Ababa.

Ghosh, D.P., 1971a. The application of linear filter theory to the direct interpretation of geoelectrical resistivity Sounding Measurements. Geophysical Prospecting 19.

Ghosh, D.P., 1971b. Inverse filter coefficients for the computation of apparent resistivity standard curves for a horizontally stratified earth Geophysical prospecting 10.

Goguel, 1976. Geothermics. McGraw- Hill, Inc, USA.

Habteab, Z., and Melese, B., 1987. Water supply investigation of Boku steam bath. Ethiopian Institute of Geological Surveys (unpublished report) Note 280, Addis Ababa.

Haebrjam, G.M., 1970. The association of resistivity soundings. Geophysical prospecting 18.

Haterton, T., Macdonald, W.j,p., and Thompson, G.E,K., 1966. ' Geophysical methods in gepthrmal prospecting in New Zealand', Bull. Volcanologoque, 29.

Mohr, P.A., 1960. Report on geological excursion through Southern Etiopia. Bull. Geophys. Observatory. n.9, 1-5, Addis Ababa.

Mohr, 1986. Sequential aspects of the tectonic evolution of Ethiopian Rift. Mem. Soc. geol. It., n.31, 447-461, Italy.

Mohr, P.A. (1971). The Geology of Ethiopia. Addis Ababa University Press.

Mohr, P.A., 1976a. The Ethiopian Rift System. Geophys. Observatory, 11, 1-65.

Mohr, P.A. (1983). Perspective on the Ethiopian volcanic province. Bull. Volcanol. 46 23-43

Orellana, E., & Mooney, H.M., 1966. Master tables & curves for vertical electrical sounding over layerd structures. Inter ciencia, Mad id.

Parasnis, D.S., 1986. Principles of applied Geophysics.Chapman and Hall. Great Britain.

Raybach,L. & Muffler, L.J.P., 1981. Geothermal systems: Principles & case histories, John Wiley & Sons Ltd.

Schlumberger, C., & Schlumberger, M., 1932. Depth of investigation attainable by potential methods electrical exploration. Geophysical Prospecting.

Skutan B . , (1982). Geophysical survey for hydrogeological study in the Nazerath area(sheet NC 37-15) . unpublished Reporet , EIGS ,Addis Ababa .

Stefanescu, S.S., & Schlumberger, C. & M., 1930. Surla distribution electrique potentielle autur d'une prise de terre poctuelle dans un terrain a couches horizontales, homogenes et isotopes. J.Phys. Radium, 7

Tamiru, A. and Vernier,A.,1997. Conceptual Model for Boku Hydrothermal area (Nazareth), Main Ethiopian Rift Valley.SINET.J.Sci.,20(2):283-291, Addis Ababa University, Addis Ababa.

Tamiru, A.,1993. Preliminary Analysis in the availability of Groundwater in Ethiopia. SINET.J.Sci.16:43-59

Tamiru a, Vernier ,A., 1995. Hydrogeology of Debre Zeit area Central part of the Main Ethiopian Rift Valley. In: Proceedings of the 2nd International Meeting for Young Researchers in Applied Geology, Oct. 10-13, 1995, 217-223. (Cuneo),Italy.

Tatsch,J.H., 1976. Geothermal Deposit. James Hendertson Tatsch, U.S.A.

Tesfaye,C., 1982. Hydrogeology of Lakes Region. Ministry of Mines and Energy, Ethiopian Institute of Geological Surveys, Memoir No. 7, p. 97, Addis Ababa, Ethiopia.

UNDP, Tech. Report., 1973. Investigation of Geothermal Resources for power development in

Woldu .A. ,(1994) ,Hydrogeology of Nazreth ,Msc.thesis ,AAU .Addis Ababa

Ethiopia, Geology, Geochemistry, and Hydrology of hot springs of the east African Rift System within Ethiopia.

DECLARATION

The thesis is my original work, has not been presented for a degree in any other university and that all sources of material used for the thesis have been duly acknowledged.